International Journal of Engineering Science

# A mechanical model for thin sheet straight cutting in the presence of an elastic support

--Manuscript Draft--

| | |
|---|---|
| **Manuscript Number:** | |
| **Article Type:** | Full Length Article |
| **Section/Category:** | Solids and Materials |
| **Keywords:** | Linear Fracture Mechanics; Foundation; Stress Intensity Factors; Thin sheet cutting |
| **Corresponding Author:** | Andrea Nobili, Ph.D.<br>Università degli Studi di Modena e Reggio Emilia: Universita degli Studi di Modena e Reggio Emilia<br>Modena, ITALY |
| **First Author:** | Timofei Shugailo |
| **Order of Authors:** | Timofei Shugailo |
| | Andrea Nobili, Ph.D. |
| | Gennady Mishuris, PhD |
| **Abstract:** | We study the mechanics of sheet straight cutting in terms of a linear elastic fracture mechanics (LEFM) problem for a infinite thin elastic Kirchhoff plate partly supported by a Winkler foundation. The plate features a semi-infinite crack that is located at the edge of the supported zone and that is subjected to shear and bending loads, representing the action of the cutting tool (e.g. scissors blades). The fact that the plate is only partly supported by the foundation significantly complicates the analysis for it creates a non-symmetric framework, both locally and globally. Yet, a semi-analytical solution is obtained through casting the matrix Wiener-Hopf problem in terms of a pair of convolution integral equations defined on a semi-infinite domain. Stress intensity factors (SIFs) are obtained which converge to the known limits for a symmetric and skewsymmetric free plate. This analysis reveals the fundamental role played by the support in affecting the SIFs in an opposing manner, by enhancing/decreasing the symmetric/skew-symmetric components. Consequently, changing the support stiffness is capable of shifting the failure mechanism, from bending to shear. This observation may be taken advantage of when cutting materials which are more sensitive to either of these failure mechanisms. Also, it proves that the role of the support cannot be neglected when developing mechanical models of any cutting process. |
| **Suggested Reviewers:** | Giuseppe Saccomandi, PhD<br>Full Professor, University of Perugia<br>giuseppe.saccomandi@unipg.it<br>Established expert in the field of solid mechanics |
| | Micheal Nieves, PhD<br>Senior Lecturer, Keele University<br>m.nieves@keele.ac.uk<br>Expert in the field of fracture mechanics |
| | Victor Eremeev<br>University of Cagliari<br>victor.eremeev@unica.it<br>Expert in the field of material fracture |

UNIMORE
UNIVERSITÀ DEGLI STUDI DI MODENA E REGGIO EMILIA

August 10th, 2023

Dear Editor,

Please find enclosed, the research paper

"A mechanical model for thin sheet straight cutting in the presence of an elastic support"
by
T. Shugailo, A. Nobili and G. Mishuris

submitted for consideration in the International Journal of Engineering Science.

The paper presents a new solution in LEFM for a crack thin plate partly supported by an elastic foundation.
To the best of the authors' knowledge, it is the first contribution that investigates the role of the (partial) support in affecting the cutting process, especially in terms of the stress intensity factor and of the corresponding failure mode of the material.
The material is original and it has not been submitted for publications in other journals.
The authors are aware of the ethical guidelines put forward by the journal and fully adhere to it.
The authors are in no conflict of interest regarding the material presented in this paper.
This version of the paper is approved by all authors.

Best regards,
Andrea Nobili
(Corresponding author)

**Highlights of the paper**
**A mechanical model for thin sheet straight cutting in the presence of an elastic support**

- We consider the role of partial elastic support in the problem of a semi-infinite linear crack located at the edge of the supported zone for a thin elastic plate
- We find that the support acts as coupling between the bending and the shearing stress intensity factors (SIFs)
- Consequently, the material failure mode is fundamentally driven by the stiffness of the support which cannot be ignored in any modelling of cutting
- The support stiffness affects the SIFs in opposing fashion, decreasing one and increasing the other
- It also determines the asymptotics of the solution in the far-field for the unsupported plate
- The limiting situation of infinite support stiffness corresponds to a free cracked plate under symmetric/skew-symmetric conditions, depending on the loading
- In no case it corresponds to a cracked plate with built-in semi-edge.

Title Page (with Author Details)

# A mechanical model for thin sheet straight cutting in the presence of an elastic support

Timofei Shugailo[b], Andrea Nobili[a,*], Gennady Mishuris[b]

[a] *Dipartimento di Ingegneria Enzo Ferrari, via Vivarelli 10, 41125 Modena, Italy*
[b] *Institute of Mathematical and Physical Sciences, Aberystwyth University, Ceredigion SY23 3BZ, Wales, UK.*

# A mechanical model for thin sheet straight cutting in the presence of an elastic support

Timofei Shugailo[b], Andrea Nobili[a,*], Gennady Mishuris[b]

[a]*Dipartimento di Ingegneria Enzo Ferrari, via Vivarelli 10, 41125 Modena, Italy*
[b]*Institute of Mathematical and Physical Sciences, Aberystwyth University, Ceredigion SY23 3BZ, Wales, UK.*

**Abstract**

We study the mechanics of sheet straight cutting in terms of a linear elastic fracture mechanics (LEFM) problem for a infinite thin elastic Kirchhoff plate partly supported by a Winkler foundation. The plate features a semi-infinite crack that is located at the edge of the supported zone and that is subjected to shear and bending loads, representing the action of the cutting tool (e.g. scissors blades). The fact that the plate is only partly supported by the foundation significantly complicates the analysis for it creates a non-symmetric framework, both locally and globally. Yet, a semi-analytical solution is obtained through casting the matrix Wiener-Hopf problem in terms of a pair of convolution integral equations defined on a semi-infinite domain. Stress intensity factors (SIFs) are obtained which converge to the known limits for a symmetric and skew-symmetric free plate. This analysis reveals the fundamental role played by the support in affecting the SIFs in an opposing manner, by enhancing/decreasing the symmetric/skew-symmetric components. Consequently, changing the support stiffness is capable of shifting the failure mechanism, from bending to shear. This observation may be taken advantage of when cutting materials which are more sensitive to either of these failure mechanisms. Also, it proves that the role of the support cannot be neglected when developing mechanical models of any cutting process.

*Keywords:* Linear Fracture Mechanics; Foundation; Stress Intensity Factors; Thin sheet cutting

## 1. Introduction

In a typical sheet cutting process, a sheet of material is divided in two parts through application of a pair of large enough forces as to cause material failure. A common example is metal sheet cutting, which usually occurs by applying a shearing force, for example through a punch, to the sheet resting on a die (in which case the process is named "punching"). This process is sometimes referred to as shearing cutting (Figure 1) and it belongs to the large family of manufacturing procedures aimed at deforming a metal, such as blanking (making holes in a sheet), bending, calendering and slitting. The same basic process occurs when tearing paper with a ruler or along a table edge, as in Figure 2, for the edge operates as the cutting tool and, most importantly, the paper has to be carefully kept well in place (like from a die) for the operation to take place smoothly.

Alternatively, a pair of blades may be used, as in familiar scissor cutting. The cutting process is generally delicate and error prone, in dependence of material flaws but also of imperfections in applying the right constraining conditions, which prove crucial [2]. In particular, it is easy to see that, at the microscale, crack formation and propagation induced by the cutting process proceed in zig-zag fashion, although this may not appear so clearly at the macroscale. However, this feature may sometimes also emerge at the macroscale, when the material crack unexpectedly deviates from the straight path. In fact, we show that this behaviour is not extraneous to the classical theory of cracks, which is traditionally based on linear elastic fracture mechanics (LEFM) results that are crucially supplemented by a local symmetry requirement to predict the crack path [14, 7]. This is well straightforward inasmuch as the geometry under consideration indeed supports such symmetry requirement, at least locally, and this is in fact the case of many fracture mechanics problems

*Corresponding author

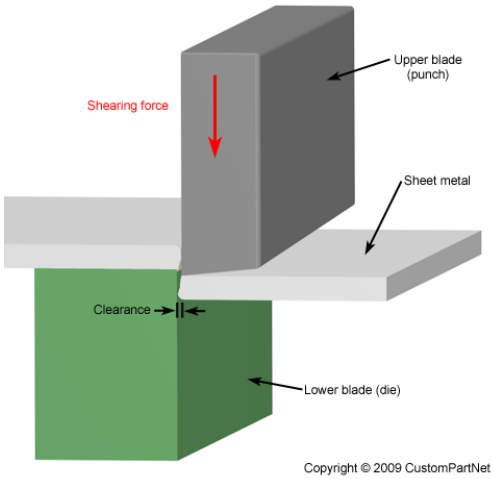


Figure 1: Skematics of shearing cutting of a steel sheet

which may be solved explicitly [1, 27, 17, 19]. Remarkably, they form the basis of many technical solutions that are applied, in the form of guidelines or codes, for the design of thin light structures, especially in the shape of shells and plates for the aerospace and high performance sectors [27, 13, 6]. The matter becomes blurred when general non-symmetric conditions are dealt with, precisely in the close neighborhood of the crack tip.

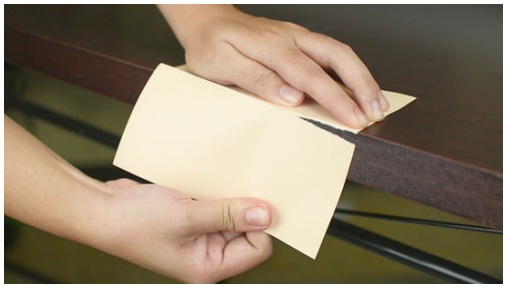

Figure 2: Tearing paper along a table edge

Clearly, the problem of cutting, even in the case of brittle materials, cannot be fully represented within the framework of LEFM, given that elasto-plastic, nonlinear, thermo-mechanical and irreversible processes may play an important role [2]. Consequently, for the full picture, numerical methods have to be reverted to in order to solve the nonlinear coupled model which emerges. However, even then, the starting point is often the stress intensity factor (SIF) of LEFM, to avoid attacking an overwhelmingly complicated problem, see, for example, [4] and [33, Chap.6]. Moreover, it is most striking that, to our best knowledge, no contributions are available in the literature which take into consideration the role of the support (the die) in affecting the mechanics of the cutting. This is all the more remarkable if one considers that any cutting, say scissor cutting, cannot take place without the action of a support, if only in consideration of the fact that cutting forces can never be fully self-equilibrated (whence the role of the clearance in Fig.1). Further, we mention that other pathways to failure exist beside cracking, as described in [32] for delamination.

Only a limited number of crack problems have been solved analytically within elastic plate theory [29], and this despite the utmost practical importance of these structures in engineering applications [15, Chap.11]. The reasons behind this shortcoming may be traced to the difficulties attached to solving a fourth order PDE with complicated boundary conditions, for which the superposition principle is of limited help. Consequently, only symmetric or skew-symmetric conditions could be solved in general [28]. When introducing an elastic foundation, matters become even more intricate, because, from a mathematical standpoint, the presence of the foundation destroys the homogeneous character of the plate PDE. In their pioneering work, [1] could

work out the SIFs in bending of a fully supported plate, that is a symmetric setting. This work was later extended to a weakly nonlocal foundation [17, 18] and then generalized to dynamical effects [19]. Incidentally, these problems are also very relevant to the engineering design of pavements [25]. The case of a finite crack and of a shell were considered by [5] and later by [16], while a simplified 3D theory was adopted in [9]. In [3], a closed-form Green function for a Griffith crack or a rigid line inclusion (anticrack) in an infinite anisotropic elastic plate could be obtained. These results were recently improved by [10] to reconcile the rigid body motions of the plate with that of the inclusion. The problem of studying the role of the foundation in affecting crack propagation is conceptually similar to that recently considered in [24], where crack penetration is antagonized by contrast in fracture toughness. In such studies, analysis of the Energy Release Rate (ERR) or, equivalently, of the SIF, plays a crucial role [23]. Moreover, specific boundary conditions may significantly influence not only the those fracture measures, but even leads to different singularities at the crack/defect tip. For example, if one considers surface stress prescribed along the body surface, the relations between the ERR and SIFs may change, as well as the stress singularity itself [8] that requires an additional separate analysis in terms of possible fracture initiation/propagation.

In this paper, we investigate the fundamental LEFM problem of an infinite thin elastic Kirchhoff plate partially supported by an elastic local (Winkler) foundation (the die). The plate sustains a semi-infinite rectilinear crack, located precisely along the foundation edge, which is loaded, in continuous fashion, at the crack flanks, to simulate the cutting tool action, for example the scissors blades. Spotlight is set on determining the stress intensity factors and, in particular, on being able to assess the role of the foundation properties on the cutting process and specifically on its path. The problem is laid out in Section 2 and then recast in the Fourier domain in Sec.3 in the form of a pair of inhomogeneous Weiner-Hopf functional equations [21]. Since the kernel matrix is non-diagonal, this coupled problem cannot be tackled in general. This difficulty is overcome first by regularization (Sec.4) and subsequently by reduction to a pair of Fredholm convolution equations (Sec.5), which are then solved numerically (Sec.6). In an attempt to lighten the mathematical structure of the manuscript, detailed derivations have been moved to the Appendix. Conclusions are drawn in Sec.7. Results compare favourably with the limiting cases of a free plate under symmetric and skew-symmetric global conditions (see Sec.Appendix A). Interestingly, the limiting case of an exceedingly stiff (weak) support does not correspond to the solution of a built-in (free) half-plate, unless special symmetries are assumed for the loading.

## 2. Governing equations

Let us consider an infinite Kirchhoff plate partially supported by a Winkler elastic foundation and partially free (Fig.3). A Cartesian reference frame is attached to the plate in such a manner that the $x$-axis coincides with the transition line at the supported/free zone. We assume that the supported plate occupies the upper half-plane A, $y > 0$, and the free plate is located in the lower half-plane B, $y < 0$. A semi-infinite rectilinear crack is located at negative values of the $x$-axis. The governing equation for the transverse

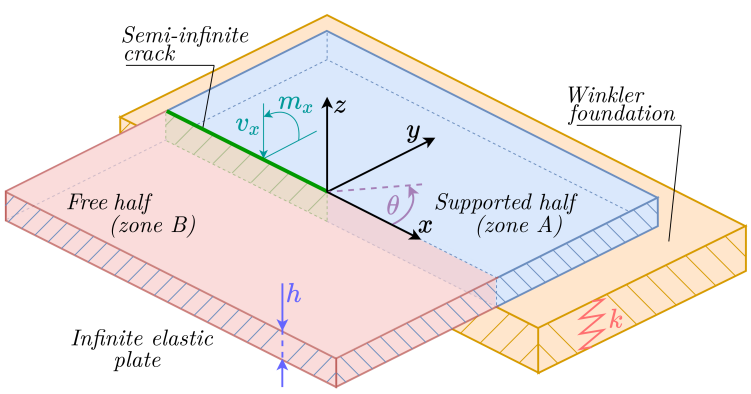


Figure 3: A Kirchhoff plate partially supported on a Winkler elastic foundation

displacement of the plate $u_z$ reads

$$D\triangle\triangle u_z = q - \pi, \tag{1}$$

being $\triangle = \partial_{xx} + \partial_{yy}$ the Laplace operator in two dimensions, $q$ the transverse distributed load, $D = Eh^3/(12(1-\nu))$ the plate bending stiffness and $\pi$ the soil reaction. Here, $E$ is Young modulus and $\nu$ Poisson's ratio. For the case at hand, the soil reaction is given by

$$\pi = \begin{cases} ku_z, & y > 0, \\ 0, & y < 0, \end{cases} \tag{2}$$

wherein $k$ is Winkler elastic modulus. Assuming no applied external loading, Eqs.(1, 2) may be rewritten as (cf.[20] in the static framework)

$$\begin{cases} \triangle\triangle u_z + \lambda^{-4} u_z = 0, & y > 0, \\ \triangle\triangle u_z = 0, & y < 0. \end{cases} \tag{3}$$

having let the plate bending length scale

$$\lambda = \sqrt[4]{\frac{D}{k}}.$$

Hereinafter, we adopt the dimensionless variables

$$(x_1, x_2, w) = \lambda^{-1}(x, y, u_z). \tag{4}$$

Besides, we denote by $w^{A,B}$ the restriction of $w$ to the domain above (below) the crack line, namely $w^{A,B}(x_1, x_2) = w(x_1, x_2)$ with $x_2 \gtrless 0$. Further, we let the dimensionless quantities: slope (along $x_2$), bending moment and Kirchhoff equivalent shearing force (acting across the crack line)

$$\begin{aligned} \phi &= \partial_{x_2} w, \\ m &= \left(\partial_{x_2 x_2} + \nu \partial_{x_1 x_1}\right) w, \\ v &= \partial_{x_2}\left[\partial_{x_2 x_2} + (2-\nu)\partial_{x_1 x_1}\right] w, \end{aligned} \tag{5}$$

where the last two have been brought in dimensionless form dividing by $D\lambda^{-1}$ and $D\lambda^{-2}$, respectively.

The boundary conditions demand continuity beyond the crack-tip

$$\left.\begin{aligned} w^A(x_1, 0) &= w^B(x_1, 0) \\ \phi^A(x_1, 0) &= \phi^B(x_1, 0) \\ m^A(x_1, 0) &= m^B(x_1, 0) \\ v^A(x_1, 0) &= v^B(x_1, 0) \end{aligned}\right\} x_1 > 0, \tag{6}$$

and a prescribed continuous (and symmetric) loading at the crack flanks

$$\left.\begin{aligned} m^A(x_1, 0) &= M_0(x_1) \\ m^B(x_1, 0) &= M_0(x_1) \\ v^A(x_1, 0) &= V_0(x_1) \\ v^B(x_1, 0) &= V_0(x_1) \end{aligned}\right\} x_1 < 0, \tag{7}$$

where it is understood that $M_0(x_1)$ and $V_0(x_1)$ are the bending moment and shearing force applied at the crack faces. Symmetry in the applied load is not really important here and it is only assumed for simplicity because, otherwise, additional balance conditions would be needed.

We further assume that the given loads are not singular and decay at infinity:

$$|M_0(x_1)|, |V_0(x_1)| < \infty, \quad x_1 \in (-\infty, 0], \tag{8}$$

and

$$M_0(x_1) = O\left(e^{\gamma_\infty x_1}\right), \quad V_0(x_1) = O\left(e^{\gamma_\infty x_1}\right), \quad x_1 \to -\infty, \tag{9}$$

$$M_0(x_1) = O\left(|x_1|^{\gamma_0}\right), \quad V_0(x_1) = O\left(|x_1|^{\gamma_0 - 1}\right), \quad x_1 \to 0^-, \tag{10}$$

where $\gamma_\infty > 0$, $\gamma_0 > 1/2$ are any constants not weaker than the specific behaviour of the solution. Those conditions may be weakened but it is not our goal in this paper.

We agree to add a subscript zero to denote the restriction of a function to the crack line $x_2 = 0$, i.e. $w_0(x_1) = w(x_1, 0)$. Clearly, Eqs.(6) and (7) imply continuity of bending moment and shearing force along the entire $x_1$ axis. Indeed, taking the difference, we get

$$[\![w]\!] = 0, \qquad [\![\phi]\!] = 0, \qquad x_1 > 0, \tag{11a}$$

$$[\![m]\!] = 0, \qquad [\![v]\!] = 0, \qquad -\infty < x_1 < \infty, \tag{11b}$$

$$m_0^B(x_1) = M_0(x_1), \qquad v_0^B(x_1) = V_0(x_1), \qquad x_1 < 0. \tag{11c}$$

where $[\![f]\!] = f_0^A - f_0^B$ at $x_2 = 0$.

Assuming sufficient decay at infinity, one can observe that the following balance conditions should be satisfied for any $x_2 \leq 0$ (that is in the free plate)

$$\int_{-\infty}^{\infty} v^B(x_1, x_2)\mathrm{d}x_1 = 0, \quad \int_{-\infty}^{\infty} m^B(x_1, x_2)\mathrm{d}x_1 = 0, \quad \int_{-\infty}^{\infty} x_1 v^B(x_1, x_2)\mathrm{d}x_1 = 0, \tag{12}$$

expressing vertical and rotational equilibrium about $x_1$ and $x_2$, respectively. In particular, along the supported/free plate transition line $x_2 = 0$, taking into account the conditions (11b), one gets

$$\int_{-\infty}^{\infty} m_0^{A,B}(x_1)\mathrm{d}x_1 = 0, \quad \int_{-\infty}^{\infty} v_0^{A,B}(x_1)\mathrm{d}x_1 = 0, \quad \int_{-\infty}^{\infty} x_1 v_0^{A,B}(x_1)\mathrm{d}x_1 = 0. \tag{13}$$

Besides, we anticipate that

$$w(r, \theta) = P_w(x_1, x_2) + r^{3/2}\left[\mathcal{K}_e w_e(\theta) + \mathcal{K}_o w_o(\theta)\right] + O\left(r^2\right), \quad \text{as } r \to 0, \tag{14}$$

where $\theta \in [-\pi, \pi]$, $\theta = \pm\pi$ corresponding to the upper/lower crack flank, and we have let the rigid body motion (rbm)

$$P_w(x_1, x_2) = \mathcal{W}_0 + \mathcal{W}_1 x_1 + \mathcal{W}_2 x_2.$$

Here, we have introduced the polar coordinates $(r, \theta)$ such that $(x_1, x_2) = r(\cos\theta, \sin\theta)$. Also, $w_{e,o}(\theta)$ is the even/odd part in $\theta$ of the first asymptotic term in the displacement [31, Eq.(8)]

$$w_e(\theta) = -\cos\frac{3\theta}{2} + \frac{3(1-\nu)}{\nu+7}\cos\frac{\theta}{2}, \quad w_o(\theta) = \sin\frac{3\theta}{2} - \frac{3(1-\nu)}{3\nu+5}\sin\frac{\theta}{2}, \tag{15}$$

where $\mathcal{K}_{e,o}$ are the normalized stress intensity factors (SIFs). From the asymptotics (14), we can easily compute the slope, bending moment and shearing force across a surface with normal in the $\theta$ direction

$$\phi_\theta(r, \theta) = \mathcal{W}_2 + r^{1/2}\Big(\mathcal{K}_e\phi_o(\theta) + \mathcal{K}_o\phi_e(\theta)\Big) + O\left(r\right), \qquad \text{as } r \to 0, \tag{16a}$$

$$m_\theta(r, \theta) = r^{-1/2}\Big(\mathcal{K}_e m_e(\theta) + \mathcal{K}_o m_o(\theta)\Big) + \mathcal{M}_0 + O\left(r^{1/2}\right), \qquad \text{as } r \to 0, \tag{16b}$$

$$v_\theta(r, \theta) = r^{-3/2}\Big(\mathcal{K}_e v_o(\theta) + \mathcal{K}_o v_e(\theta)\Big) + \mathcal{V}_1 r^{-1} + O\left(r^{-1/2}\right), \qquad \text{as } r \to 0, \tag{16c}$$

where

$$\phi_e(\theta) = \frac{3}{2}\Big(\cos\frac{3\theta}{2} - \frac{1-\nu}{3\nu+5}\cos\frac{\theta}{2}\Big), \qquad \phi_o(\theta) = \frac{3}{2}\Big(\sin\frac{3\theta}{2} - \frac{1-\nu}{\nu+7}\sin\frac{\theta}{2}\Big),$$

$$m_e(\theta) = \frac{3}{4}(1-\nu)\Big(\cos\frac{3\theta}{2} + \frac{3\nu+5}{\nu+7}\cos\frac{\theta}{2}\Big), \qquad m_o(\theta) = -\frac{3}{4}(1-\nu)\Big(\sin\frac{3\theta}{2} + \sin\frac{\theta}{2}\Big),$$

$$v_e(\theta) = -\frac{3}{8}(1-\nu)\Big(\cos\frac{3\theta}{2} + \frac{\nu+7}{3\nu+5}\cos\frac{\theta}{2}\Big), \qquad v_o(\theta) = -\frac{3}{8}(1-\nu)\Big(\sin\frac{3\theta}{2} + \sin\frac{\theta}{2}\Big).$$

As well known, the squares of $\mathcal{K}_{e,o}$ are proportional to the energy release rate.

### 2.1. Apriori asymptotic estimate of the solution components at infinity

To deliver the unique solution to the problem, we demand that it decays within the supported plate as

$$w^A(r,\theta) \sim \phi^A(r,\theta) = O(r^{-5/2}), \quad \theta \in [0,\pi], \quad \text{as } r \to +\infty, \tag{18}$$

whence, by continuity, the same occurs in the free plate at $\theta = 0$. Motivation of these assumptions is given in Sec.Appendix C.1. Conversely, little knowledge is available concerning the behaviour of the solution in the free plate outside the line $\theta = 0$. For this reason, we look at some auxiliary problems which emerge from taking symmetric or anti-symmetric conditions (see Appendix Appendix A). From these, we deduce

$$w^B(r,-\pi) = W_1^\infty r + W_2^\infty + O(r^{-1/2}), \quad \text{as } r \to +\infty, \tag{19a}$$

$$\phi^B(r,-\pi) = \Psi_1^\infty \log r + \Psi_2^\infty + O(r^{-1/2}), \quad \text{as } r \to +\infty, \tag{19b}$$

where the constants (which may also vanish) are to be found in the following. The corresponding estimates for the jumps across the crack line easily follow, also in light of the fact that all functions vanish at infinity in the supported zone, namely

$$[\![w]\!] = \Phi_0 x_1 - W_0^\infty + O(|x_1|^{-1/2}), \quad [\![\phi]\!] = \Psi_0(|x_1|)^{1/2} + O(|x_1|^{-1/2}), \quad x_1 \to -\infty. \tag{20}$$

Furthermore, we point out that those estimates emerge by assuming the fastest growing scenario, and may well be slower than assumed, also in dependence of the applied loading. Yet, for specific external forces, these estimates may be sharpened at the expense of generality. Instead, we prefer to stick with general results to show that the solution technique does not rely on specific assumptions on the given functions.

For the remaining two unknowns

$$m(r,\theta) = O(r^{-5/2}), \quad v(r,\theta) = O(r^{-7/2}), \quad \theta \in (-\pi,0), \quad \text{as } r \to +\infty. \tag{21}$$

Having all these information in place, we are now in position to develop solution to the problem. For this, we move to the Fourier space and use Abelian- and Tiberian-type of theorems [22] to evaluate the corresponding asymptotic behavior for the unknowns.

## 3. Application of the Fourier transform and asymptotics of the Fourier images

### 3.1. Fourier analysis of the general equations

In the following, we take advantage of the Fourier transform method, which has proven extremely useful in several problems dealing with continuum as well as discrete media (and even for hybrid solids, see [30]). We therefore introduce the (two-sided or bilateral) Fourier transform

$$\bar{w}(s,x_2) = \int_{-\infty}^{\infty} w(x_1,x_2)\exp(\mathrm{i}sx_1)\mathrm{d}x_1, \tag{22}$$

alongside the half-transforms

$$\bar{w}^{\pm}(s,x_2) = \int_{-\infty}^{\infty} w_{\pm}(x_1,x_2)\exp(\mathrm{i}sx_1)\mathrm{d}x_1, \tag{23}$$

where $w_{\pm}(x_1,x_2) = H(\pm x_1)w(x_1,x_2)$ and $H(x_1)$ is Heavyside's step function. Immediately, we have

$$\bar{w}(s,\cdot) = \bar{w}^+(s,\cdot) + \bar{w}^-(s,\cdot). \tag{24}$$

In the same way we denote the Fourier transforms of the remaining fields $\phi$, $m$ and $v$, noting only that, for the last, the respective integral should be treated in the sense of distributions.

We are now in a position to take the Fourier transform of the transmission conditions (11a,11b)

$$[\![\bar{w}^+]\!] = [\![\bar{\phi}^+]\!] = [\![\bar{m}]\!] = [\![\bar{v}]\!] = 0, \tag{25}$$

whence, clearly,

$$[\![\bar{w}]\!] = [\![\bar{w}^-]\!], \quad [\![\bar{\phi}]\!] = [\![\bar{\phi}^-]\!]. \tag{26}$$

In similar fashion, the balance conditions (13) may be rewritten as

$$\bar{m}_0^A(0) = \bar{m}_0^B(0) = \bar{v}_0^A(0) = \bar{v}_0^B(0) = \frac{\mathrm{d}\bar{v}_0^A}{\mathrm{d}s}(0) = \frac{\mathrm{d}\bar{v}_0^B}{\mathrm{d}s}(0) = 0, \tag{27}$$

where the notation $f_0^{A,B}$ stands for

$$f_0^A(\cdot) = \lim_{x_2 \to 0+} f^A(\cdot, x_2), \quad f_0^B(\cdot) = \lim_{x_2 \to 0-} f^B(\cdot, x_2).$$

Besides, we recall the inverse Fourier transform

$$\left[w, w_+, w_-\right](x_1, x_2) = (2\pi)^{-1} \int_{-\infty}^{\infty} \left[\bar{w}, \bar{w}^+, \bar{w}^-\right](s, x_2) \exp(-\mathrm{i}sx_1)\mathrm{d}s. \tag{28}$$

Taking the bilateral Fourier transform along $x_1$ of the first of Eqs.(3) lends a linear constant coefficient ODE whose general solution is

$$\bar{w}^A(s, x_2) = A_1 e^{-\alpha_1 x_2} + A_2 e^{-\alpha_2 x_2}, \quad \alpha_j = \sqrt{s^2 + \mathrm{i}(-1)^j}, \quad j = 1, 2, \quad x_2 > 0, \tag{29}$$

where $A_j = A_j(s)$ and i is the imaginary unit, i.e. $\mathrm{i}^2 = -1$. Here, provision should be taken so that the square roots lend positive real values on the real axis and branch cuts are not intersecting the real axis (for example, branch cuts may be taken parallel to the imaginary axis, see [21]). Denoting by $z^* = \Re(z) - \mathrm{i}\Im(s)$ the complex conjugate of $z = \Re(z) + \mathrm{i}\Im(s)$, we have

$$\alpha_1(0) = \alpha_2^*(0) = e^{-\mathrm{i}\pi/4}, \tag{30}$$

so that $\alpha_{1,2}^2(0) = \mp\mathrm{i}$. Similarly, the solution of the second of Eqs.(3) reads (free domain)

$$\bar{w}^B(s, x_2) = (B_1 + x_2 B_2) \exp(\beta x_2), \quad x_2 < 0, \tag{31}$$

and it is understood that $B_j = B_j(s)$ $(j = 1, 2)$ and we have $\beta(s) = \sqrt{s^2}$ such that $\operatorname{sign} s = \beta(s)/s$ for $s \in \mathbb{R}$. Moreover, to prevent having branch cuts reaching the real axis, we may perturb $\beta(s) = \lim_{\epsilon \to 0} \sqrt{s^2 + \epsilon^2}$ so that no zero sits right on the real axis [21]. With this, we are now able to introduce the splitting

$$\beta(s) = \beta^+(s)\beta^-(s), \quad \beta^+(s) = \sqrt{0 - \mathrm{i}s}, \quad \beta^-(s) = \sqrt{0 + \mathrm{i}s}, \tag{32}$$

where we take the standard definition of the square root with the cut on the negative part of real axis. It is emphasized that Fourier transforms are defined on the real axis only, but can be extended by analytic continuation into the complex plane.

In terms of the general solution, we have, in the supported plate $x_2 \geq 0$,

$$\bar{\phi}^A(s, x_2) = -\alpha_1 A_1 e^{-\alpha_1 x_2} - \alpha_2 A_2 e^{-\alpha_2 x_2}, \tag{33a}$$

$$\bar{m}^A(s, x_2) = A_1 e^{-\alpha_1 x_2} \left(\alpha_1^2 - \nu s^2\right) + A_2 e^{-\alpha_2 x_2} \left(\alpha_2^2 - \nu s^2\right), \tag{33b}$$

$$\bar{v}^A(s, x_2) = -\alpha_1 A_1 e^{-\alpha_1 x_2} \left(\alpha_1^2 + (\nu - 2)s^2\right) - \alpha_2 A_2 e^{-\alpha_2 x_2} \left(\alpha_2^2 + (\nu - 2)s^2\right), \tag{33c}$$

and in the free plate $x_2 \leq 0$

$$\bar{\phi}^B(s, x_2) = e^{\beta x_2} \left[\beta \left(B_2 x_2 + B_1\right) + B_2\right], \tag{34a}$$

$$\bar{m}^B(s, x_2) = e^{\beta x_2} \left[-(\nu - 1)s^2 \left(B_2 x_2 + B_1\right) + 2\beta B_2\right], \tag{34b}$$

$$\bar{v}^B(s, x_2) = e^{\beta x_2} \left[\beta(\nu - 1)s^2 \left(B_2 x_2 + B_1\right) + B_2(\nu + 1)s^2\right]. \tag{34c}$$

Finally, substituting (33) and (34) into the transmission conditions (25), we have:

$$[\![\bar{w}]\!] = A_1(s) + A_2(s) - \beta^{-1} B_*(s) = [\![\bar{w}^-]\!], \tag{35a}$$

$$[\![\bar{\phi}]\!] = -\alpha_1 A_1(s) - \alpha_2 A_2(s) - B_*(s) - B_2(s) = [\![\bar{\phi}^-]\!], \tag{35b}$$

$$0 = (\alpha_1^2 - \nu s^2) A_1(s) + (\alpha_2^2 - \nu s^2) A_2(s) + (\nu - 1)\beta B_*(s) - 2\beta B_2(s), \tag{35c}$$

$$0 = -\alpha_1(\alpha_1^2 + (\nu - 2)s^2) A_1(s) - \alpha_2(\alpha_2^2 + (\nu - 2)s^2) A_2(s) - (\nu - 1)s^2 B_*(s) - (\nu + 1)s^2 B_2(s), \tag{35d}$$

having introduced the convenient shorthand (see Appendix B).

$$B_*(s) \equiv \beta(s) B_1(s). \tag{36}$$

In the equations above (33) – (36), it is understood that $\alpha_j = \alpha_j(s), \beta = \beta(s)$ and $s \in \mathbb{R}$, while (35a) and (35b) can be analytically extended into the complex half-plane $s \in \mathbb{C}^-$.

### *3.2. Derivation of the Wiener-Hopf system*

In light of (25), the boundary conditions (7) reads

$$\bar{m}_0^-(s) \equiv \bar{m}_0^{A,B\,-}(s) = \bar{M}_0^-(s), \tag{37a}$$

$$\bar{v}_0^-(s) \equiv \bar{v}_0^{A,B\,-}(s) = \bar{V}_0^-(s). \tag{37b}$$

We consider the linear system of algebraic equations (35) in the unknowns $A_1, A_2, B_1, B_2$. This system is regular, because its determinant has no zeros. Upon solving these unknowns in terms of $[\![\bar{w}^-]\!]$ and $[\![\bar{\phi}^-]\!]$ and then plugging the result into (37), we get the system of inhomogenenous functional equations of the Wiener-Hopf type

$$\begin{cases} -K_{11}[\![\bar{\phi}^-]\!] + K_{12}[\![\bar{w}^-]\!] = \bar{m}_0{}^+ + \bar{M}_0^-(s), \\ -K_{12}[\![\bar{\phi}^-]\!] + s^2 K_{22}[\![\bar{w}^-]\!] = \bar{v}_0{}^+ + \bar{V}_0^-(s), \end{cases} \tag{38}$$

where

$$\begin{aligned} \delta_0 K_{11} &= (1-\nu)s^4\left[(\alpha_1+\alpha_2)(3+\nu) + 2(1+\nu)\beta\right] + 4(1-\nu)s^2\alpha_1\alpha_2\beta + 2\beta, \\ \delta_0 K_{12} &= s^2\left\{(1-\nu)^2\left(s^2 - \alpha_1\alpha_2\right)s^2 + 1 + \nu\right\}, \\ \delta_0 K_{22} &= \delta_0 K_{11} + \mathrm{i}(1-\nu)(3+\nu)s^2(\alpha_1 - \alpha_2), \end{aligned}$$

and having let

$$\delta_0(s) = (\alpha_1(s) + \beta(s))^2(\alpha_2(s) + \beta(s))^2. \tag{39}$$

It is observed that, when the plate is everywhere free, that is for $\lambda \to \infty$, the system (38) decouples owing to symmetry, i.e. $K_{12} \to 0$. Besides, it is $K_{11} \to K_{22}$.

At the origin, we have the following asymptotics for the components, that are even functions of $s \in \mathbb{R}$,

$$\left.\begin{aligned} K_{11} = K_{22} &= 2\beta(s)\big(1 + O(\beta(s))\big) \\ K_{12} &= (1+\nu)s^2\big(1 + O(\beta(s))\big) \end{aligned}\right\} \text{ as } s \to 0, \tag{40}$$

thus, by (Appendix C.13,Appendix C.36), we get asymptotic consistency at zero

$$\begin{aligned} &K_{11}[\![\bar{\phi}^-]\!] = O(s^{3/2}), \quad K_{12}[\![\bar{w}^-]\!] = O(s^{3/2}), \qquad \bar{m}_0{}^+ + \bar{M}_0^-(s) = O(s^{3/2}), \\ &K_{12}[\![\bar{\phi}^-]\!] = O(s^{5/2}), \quad s^2K_{22}[\![\bar{w}^-]\!] = O(s^{5/2}), \quad \bar{v}_0{}^+ + \bar{V}_0^-(s) = O(s^{5/2}), \end{aligned} \qquad s \to 0.$$

We point out that individual terms at RHS of (38) have different asymptotics than their sum, namely

$$\bar{m}_0^+(s), \bar{M}_0^-(s), \bar{v}_0^+(s), \bar{V}_0^-(s) = O(1), \quad s \to 0, \tag{41}$$

as it appears from (Appendix C.35a,Appendix C.35b). Indeed, this result comes from the balance conditions (27)

$$\bar{m}_0^+(0) + \bar{M}_0^-(0) = \bar{v}_0^+(0) + \bar{V}_0^-(0) = \frac{\mathrm{d}\bar{v}_0^+}{\mathrm{d}s}(0) + \frac{\mathrm{d}\bar{V}_0^-}{\mathrm{d}s}(0) = 0, \tag{42}$$

and accounting for (Appendix C.12)

$$\frac{\mathrm{d}\bar{m}_0^+}{\mathrm{d}s}(0) + \frac{\mathrm{d}\bar{M}_0^-}{\mathrm{d}s}(0) = \frac{\mathrm{d}^2\bar{v}_0^+}{\mathrm{d}s^2}(0) + \frac{\mathrm{d}^2\bar{V}_0^-}{\mathrm{d}s^2}(0) = 0. \tag{43}$$

At infinity we have

$$\left.\begin{aligned} K_{11} = K_{22} &= c\beta(s) + O(s^{-3}) \\ K_{12} &= \tfrac{1+4\nu-\nu^2}{32} s^{-2} + O(s^{-6}) \end{aligned}\right\} \text{ as } |s| \to +\infty, \tag{44}$$

where we have let

$$c = \tfrac{1}{4}(1-\nu)(3+\nu). \tag{45}$$

Besides, from (Appendix C.37c,Appendix C.37d), it is

$$s\bar{m}_0^+(s) \sim \bar{v}_0^+(s) = O(s^{1/2}), \quad s\bar{M}_0^-(s) \sim \bar{V}_0^-(s) = O(s^{-\gamma_0}), \quad |s| \to \infty \text{ and } \gamma_0 > 1/2.$$

Thus, by (Appendix C.39), we see that diagonal terms asymptotics match that of the RHS

$$\begin{aligned} &K_{11}[\![\bar{\phi}^-]\!] = O(s^{-1/2}), \quad K_{12}[\![\bar{w}^-]\!] = O(s^{-9/2}), \quad \bar{m_0}^+ + \bar{M}_0^-(s) = O(s^{-1/2}), \\ &K_{12}[\![\bar{\phi}^-]\!] = O(s^{-7/2}), \quad s^2K_{22}[\![\bar{w}^-]\!] = O(s^{1/2}), \quad \bar{v_0}^+ + \bar{V}_0^-(s) = O(s^{1/2}), \end{aligned} \quad s \to \infty. \tag{46}$$

Besides, for the determinant we have

$$\Delta(s) = K_{12}^2 - s^2K_{11}K_{22} = -4cs^4\delta_0^{-1}\big(\left(1-\nu^2\right)s^4 + 2\alpha_1\alpha_2(1-\nu)s^2 + 1\big), \tag{47}$$

whence

$$\Delta(s) = 4cs^4 + O(s^6), \qquad s \to 0, \tag{48}$$

$$\Delta(s) = c^2s^4 + O(s^2), \qquad s \to \infty. \tag{49}$$

Thus, the determinant of this Wiener-Hopf system tends to zero both as $s \to 0$ and as $s \to \infty$, which fact suggests that the unknown quantities are not properly normalized. Consequently, in the following, we transform the system (38) so that it has total index zero and both partial indices also equal to zero.

## 4. Regularization of the Wiener-Hopf system

Let's transform the system (38) by dividing the first equation by $\beta$ and the second by $s\beta$

$$\begin{cases} \beta^{-1}K_{11}\bar{h}_1^- + (s\beta)^{-1}K_{12}\bar{h}_2^- = \beta^{-1}\left(\bar{m}_0^+ + \bar{M}_0^-\right), \\ (s\beta)^{-1}K_{12}\bar{h}_1^- + \beta^{-1}K_{22}\bar{h}_2^- = (s\beta)^{-1}\left(\bar{v}_0^+ + \bar{V}_0^-\right), \end{cases} \tag{50}$$

where we have let the new unknowns

$$\bar{h}_1^-(s) = -[\![\bar{\phi}^-]\!], \quad \bar{h}_2^-(s) = s[\![\bar{w}^-]\!].$$

For these, recalling (26) and using (Appendix C.36,Appendix C.39), we get the in their domains of analyticity:

$$\bar{h}_1^-(s) \sim \bar{h}_2^-(s) = O(s^{1/2}), \qquad s \to 0, \tag{51a}$$

$$\bar{h}_1^-(s) \sim \bar{h}_2^-(s) = O(s^{-3/2}), \qquad s \to \infty. \tag{51b}$$

Similarly, by (40),

$$\left.\begin{aligned} \beta^{-1}K_{11} = \beta^{-1}K_{22} &= 2 + O(\beta(s)), \\ (s\beta)^{-1}K_{12} &= (1+\nu)\operatorname{sign} s + O(s), \end{aligned}\right\} \text{ as } s \to 0, \tag{52}$$

whence terms in the W-H system have the following balanced asymptotics at zero

$$\left.\begin{aligned} &\beta^{-1}K_{11}\bar{h}_1^-(s) = O(s^{1/2}), \quad (s\beta)^{-1}K_{12}\bar{h}_2^-(s) = O(s^{1/2}), \quad \beta^{-1}\left(\bar{m}_0^+(s) + \bar{M}_0^-(s)\right) = O(s^{1/2}), \\ &(s\beta)^{-1}K_{12}\bar{h}_1^-(s) = O(s^{1/2}), \quad \beta^{-1}K_{22}\bar{h}_2^-(s) = O(s^{1/2}), \quad (s\beta)^{-1}\left(\bar{v}_0^+(s) + \bar{V}_0^-(s)\right) = O(s^{1/2}), \end{aligned}\right\} \quad s \to 0.$$

Likewise, at infinity, we have, by (44),

$$\left.\begin{aligned} \beta^{-1}K_{11} = \beta^{-1}K_{22} &= c + O(s^{-4}), \\ (s\beta)^{-1}K_{12} &= \tfrac{1+4\nu-\nu^2}{32}s^{-4}\operatorname{sign} s + O(s^{-7}\beta), \end{aligned}\right\} \text{ as } |s| \to +\infty. \tag{53}$$

whereby

$$\left.\begin{aligned} &\beta^{-1}K_{11}\bar{h}_1^-(s) = O(s^{-3/2}), && (s\beta)^{-1}K_{12}\bar{h}_2^-(s) = O(s^{-11/2}), && \beta^{-1}\big(\bar{m}_0^+(s) + \bar{M}_0^-(s)\big) = O(s^{-3/2}), \\ &(s\beta)^{-1}K_{12}\bar{h}_1^-(s) = O(s^{-11/2}), && \beta^{-1}K_{22}\bar{h}_2^-(s) = O(s^{-3/2}), && (s\beta)^{-1}\big(\bar{v}_0^+(s) + \bar{V}_0^-(s)\big) = O(s^{-3/2}), \end{aligned}\right\} \quad s \to \infty.$$

In anticipation of splitting plus and minus terms in (50), we need to make sure that, besides *their sum*, also *each individual term at RHS* is well behaved. To this effect, we set

$$\bar{m}_*^+(s) = \bar{m}_0^+(s) + \frac{\bar{M}_0^-(0) + sq_m}{(1-\mathrm{i}s)^{\zeta_M}}, \quad \bar{M}_*(s) = \bar{M}_0^-(s) - \frac{\bar{M}_0^-(0) + sq_m}{(1-\mathrm{i}s)^{\zeta_M}}, \tag{54}$$

and

$$\bar{v}_*^+(s) = \bar{v}_0^+(s) + \frac{\bar{V}_0^-(0) + sq_{v1} + s^2q_{v2}}{(1-\mathrm{i}s)^{\zeta_V}}, \quad \bar{V}_*(s) = \bar{V}_0^-(s) - \frac{\bar{V}_0^-(0) + sq_{v1} + s^2q_{v2}}{(1-\mathrm{i}s)^{\zeta_V}}. \tag{55}$$

Here, $\zeta_M, \zeta_V > \gamma_0 + 2$ are some constants, to be specified later for convenience, which warrant fast enough decay at infinity. The important point here is that, with these definitions, the starred unknowns $\bar{m}_*^+(s)$ and $\bar{v}_*^+(s)$ preserve the same plus character as well as behaviour at infinity of the original variables $\bar{m}_0^+(s)$ and $\bar{v}_0^+(s)$, respectively. Furthermore, $\bar{m}_*^+(s)$ and $\bar{v}_*^+(s)$ satisfy the same balance conditions (42,43) as $\bar{m}(s)$ and $\bar{v}(s)$. This is achieved by simply letting

$$q_m = -\mathrm{i}\zeta_M\bar{M}_0^-(0) + \frac{\mathrm{d}\bar{M}_0^-}{\mathrm{d}s}(0), \quad q_{v1} = -\mathrm{i}\zeta_V\bar{V}_0^-(0) + \frac{\mathrm{d}\bar{V}_0^-}{\mathrm{d}s}(0), \tag{56}$$

$$q_{v2} = \frac{1}{2}\Big(\zeta_V(1-\zeta_V)\bar{V}_0^-(0) - 2\mathrm{i}\zeta_V\frac{\mathrm{d}\bar{V}_0^-}{\mathrm{d}s}(0) + \frac{\mathrm{d}^2\bar{V}_0^-}{\mathrm{d}s^2}(0)\Big), \tag{57}$$

having used (42), (43) to rewrite the last terms at RHS in terms of the applied load. With such provisions and recalling (Appendix C.35), (Appendix C.37), (Appendix C.38), we obtain the asymptotics of each term

$$s\bar{m}_*^+(s), \bar{v}_*^+(s) = O(s^{5/2}), \qquad s\bar{M}_*(s), \bar{V}_*(s) = O(s^3), \qquad s \to 0, \tag{58a}$$

$$s\bar{m}_*^+(s), \bar{v}_*^+(s) = O(s^{-1/2}), \qquad s\bar{M}_*(s), \bar{V}_*(s) = O(s^{-\gamma_0}), \qquad s \to \pm\infty. \tag{58b}$$

Therefore, the W-H system now reads

$$\begin{cases} \beta^{-1}K_{11}\bar{h}_1^- + (s\beta)^{-1}K_{12}\bar{h}_2^- = \beta^{-1}\big(\bar{m}_*^+ + \bar{M}_*\big), \\ (s\beta)^{-1}K_{12}\bar{h}_1^- + \beta^{-1}K_{22}\bar{h}_2^- = (s\beta)^{-1}\big(\bar{v}_*^+ + \bar{V}_*\big), \end{cases}$$

that, multiplying through by $\beta^-$, becomes

$$\begin{cases} \beta^{-1}K_{11}\hat{h}_1^- + (s\beta)^{-1}K_{12}\hat{h}_2^- = \hat{m}_*^+ + \hat{M}_*, \\ (s\beta)^{-1}K_{12}\hat{h}_1^- + \beta^{-1}K_{22}\hat{h}_2^- = \hat{v}_*^+ + \hat{V}_*, \end{cases} \tag{59}$$

having lumped minus terms together in the new unknowns

$$\hat{h}_{1,2}^-(s) = \beta^-(s)\bar{h}_{1,2}^-(s), \tag{60}$$

and similarly for the plus terms at RHS

$$\hat{m}_*^+ = \frac{1}{\beta^+}\bar{m}_*^+, \quad \hat{v}_*^+ = \frac{1}{s\beta^+}\bar{v}_*^+, \quad \hat{M}_* = \frac{1}{\beta^+}\bar{M}_*, \quad \hat{V}_* = \frac{1}{s\beta^+}\bar{V}_*. \tag{61}$$

The relative estimates are easily obtained from (51) and (58),

$$\hat{h}_1^-(s), \hat{h}_2^-(s), \hat{m}_*^+(s), \hat{v}_*^+(s) = O(s), \quad s \to 0, \tag{62}$$

$$\hat{h}_1^-(s), \hat{h}_2^-(s), \hat{m}_*^+(s), \hat{v}_*^+(s) = O(s^{-1}), \quad s \to \infty, \tag{63}$$

while the terms representing the applied loading $\bar{M}_*(s)$ and $\bar{V}_*(s)$ behave better than the unknown functions in the W-H system at both zero and infinity. As a result, we eventually arrive at the vectorial Wiener-Hopf problem:

$$\mathbf{N}(s)\boldsymbol{H}^-(s) + \boldsymbol{H}^+(s) = \boldsymbol{F}(s), \tag{64}$$

where

$$\boldsymbol{H}^-(s) = c[\hat{h}_1^-, \hat{h}_2^-], \quad \boldsymbol{H}^+(s) = -[\hat{m}_*^+, \hat{v}_*^+], \quad \boldsymbol{F}(s) = [\hat{M}_*, \hat{V}_*], \tag{65}$$

and clearly

$$\mathbf{N}(s) = c^{-1} \begin{bmatrix} \beta^{-1}K_{11} & (s\beta)^{-1}K_{12} \\ (s\beta)^{-1}K_{12} & \beta^{-1}K_{22} \end{bmatrix}. \tag{66}$$

.

The matrix $\mathbf{N}(s)$ has the following asymptotics at zero

$$\mathbf{N}_0(s) = 2c^{-1} \begin{bmatrix} 1 + O(\beta) & \frac{1}{2}(1+\nu)\frac{s}{\beta} + O(s) \\ \frac{1}{2}(1+\nu)\frac{s}{\beta} + O(s) & 1 + O(\beta) \end{bmatrix}, \quad s \to 0, \tag{67}$$

and at infinity

$$\mathbf{N}_\infty(s) = \mathbf{I} + O\left(s^{-4}\right), \quad s \to \infty. \tag{68}$$

The determinant of this matrix is different from zero along the closed real axis (including infinity) and it is an even function. As a result, by Gohberg and Krein's theorem (see for example, [26]), the index of the matrix is equal to zero (ind $\det \mathbf{N} = 0$). Next, the matrix $\mathbf{N}(s)$ is symmetric and even on the main diagonal and odd on the off-diagonal terms, thus it is also positive definite. As a result, its partial indices are both equal to zero. The unknowns components asymptotics at infinity along the real axis are related to the SIFs as follows:

$$H_1^-(s),\ -H_1^+(s) \sim \pm 12\sqrt{\pi}e^{\mathrm{i}\pi/4}\mathcal{K}_e \frac{c}{7+\nu}|s|^{-1}, \quad s \to \pm\infty, \tag{69a}$$

$$H_2^-(s),\ -H_2^+(s) \sim \pm 12\sqrt{\pi}e^{-\mathrm{i}\pi/4}\mathcal{K}_o \frac{c}{5+3\nu}|s|^{-1}, \quad s \to \pm\infty. \tag{69b}$$

## 5. Transformation to a system of Fredholm convolution equations

Note that due to the estimate of the sought for solution of the W-H equation (64), there exists a vector function $\mathbf{h} \in L_1(\mathbb{R})$ such that

$$\mathcal{F}\mathcal{P}_\pm \boldsymbol{h} = \boldsymbol{H}^\pm, \tag{70}$$

and this function is unique. Here, as usual, $\mathcal{F}$ is the full Fourier transform and $\mathcal{P}_\pm$ are the projectors defined through multiplication by the characteristic functions $H(x)$ and $1 - H(x)$ of the respective half axes $\mathbb{R}_\pm$. We note that $\mathcal{P}_+ + \mathcal{P}_-$ is the identity operator thus, using (70), the system (64) takes the form

$$\mathcal{F}\boldsymbol{h}(s) + (\mathbf{N}(s) - \mathbf{I})\mathcal{F}\mathcal{P}_-\boldsymbol{h}(s) = \boldsymbol{F}(s).$$

Applying now the inverse Fourier transform (28), we get

$$\boldsymbol{h}(\xi) + \mathcal{F}^{-1}\left[(\mathbf{N}(s) - \mathbf{I})\mathcal{F}\mathcal{P}_-\boldsymbol{h}(s)\right](\xi) = \boldsymbol{g}(\xi) \equiv \mathcal{F}^{-1}[\boldsymbol{F}(s)](\xi). \tag{71}$$

Reversing the order of the integration on application of Fubini's theorem, Eq.(71) may be rewritten as an integral equation of the second kind, namely

$$\boldsymbol{h}(\xi) + \int_{-\infty}^{0} \mathbf{K}(\xi - y)\boldsymbol{h}(y)\mathrm{d}y = \boldsymbol{g}(\xi), \quad \xi \in \mathbb{R}, \tag{72}$$

where the kernel is the well defined and easily computed matrix-function

$$\mathbf{K}(\lambda) = \frac{1}{2\pi}\int_{-\infty}^{\infty} \big(\mathbf{N}(s) - \mathbf{I}\big) e^{-\mathrm{i}\lambda s}\mathrm{d}s.$$

**Remark**. Interestingly, to solve the integral equation (72) we begin by considering the half-axis $x \in \mathbb{R}_-$ and, once the solution $\boldsymbol{h}_*(x)$ is obtained there, it may be extended to the positive half-axis by direct computation, in a sort of post-processing stage, through

$$\boldsymbol{h}(\xi) = \boldsymbol{g}(\xi) - \int_{-\infty}^{0} \mathbf{K}(\xi - y)\boldsymbol{h}(y)\mathrm{d}y, \quad \xi \in \mathbb{R}_+.$$

In contrast, when considering the classical approach to systems of integral equations defined on either half axis, one moves in the opposite direction to reduce it in Wiener-Hopf form, namely one needs to introduce an auxiliary function on the other half-axis and then one transforms the system to have a difference kernel.

To establish a link between the solution of the system of integral equations (72) and the SIFs we integrate by parts

$$H^- = \int_{-\infty}^{0} h(x)e^{\mathrm{i}sx}\mathrm{d}x = \frac{h(x)}{\mathrm{i}s}e^{\mathrm{i}sx}\Big|_{-\infty}^{0} - \frac{1}{\mathrm{i}s}\int_{-\infty}^{0}\frac{\mathrm{d}h}{\mathrm{d}x}(x)e^{\mathrm{i}sx}\mathrm{d}x = \mp\mathrm{i}h(0)|s|^{-1} + o(s^{-1}), \quad s \to \pm\infty,$$

$$H^+ = \int_{0}^{\infty} h(x)e^{\mathrm{i}sx}\mathrm{d}x = \frac{h(x)}{\mathrm{i}s}e^{\mathrm{i}sx}\Big|_{0}^{\infty} - \frac{1}{\mathrm{i}s}\int_{0}^{-\infty}\frac{\mathrm{d}h}{\mathrm{d}x}(x)e^{\mathrm{i}sx}\mathrm{d}x = \pm\mathrm{i}h(0)|s|^{-1} + o(s^{-1}), \quad s \to \pm\infty,$$

and, upon recalling asymptotic relationships (69), we get the sought for relationships:

$$h_1(0) = -12e^{-\mathrm{i}\pi/4}\frac{c\sqrt{\pi}}{7+\nu}\mathcal{K}_e, \quad h_2(0) = 12e^{\mathrm{i}\pi/4}\frac{c\sqrt{\pi}}{5+3\nu}\mathcal{K}_o. \tag{73}$$

## 6. Numerical solution

Let us assume for the dimensionless crack loading

$$M_0(x_1) = \frac{\lambda M_y^d}{D} = C_m\zeta f_m(-\zeta x_1), \quad V_0(x_1) = \frac{\lambda^2 V_y^d}{D} = C_v\zeta^2 f_m(-\zeta x_1), \quad x_1 < 0, \tag{74}$$

where $M_y^d$ and $V_y^d$ are the *dimensional* bending moment and shearing force applied at the crack line in terms of the dimensional coordinate $x$

$$M_y^d = Q_m f_m\left(-\frac{x}{x_0}\right), \quad V_y^d = Q_v f_v\left(-\frac{x}{x_0}\right), \quad x < 0. \tag{75}$$

Clearly, the constants $Q_m$ and $Q_v$ have dimensions of force and force over length, respectively, and they are brought in dimensionless form as $C_m = Q_m x_0 D^{-1}$ and $C_v = Q_v x_0^2 D^{-1}$. Here, we have introduced the dimensionless parameter $\zeta$

$$\lambda = x_0\zeta, \quad \text{or, equivalently,} \quad k = \frac{D}{x_0^4}\zeta^{-4} \equiv k_0\zeta^{-4}, \tag{76}$$

$x_0 > 0$ being a reference length. We point out that, due to the introduced normalisation, the original dimensional stress intensity factors $K_e^d$, $K_o^d$ are related to their dimensionless counterparts through

$$\frac{\sqrt{x_0}}{D}K_e^d = \zeta^{-1/2}\mathcal{K}_e(\zeta), \quad \frac{\sqrt{x_0}}{D}K_o^d = \zeta^{-1/2}\mathcal{K}_o(\zeta). \tag{77}$$

In the following, we consider two cases, namely $C_m = 1$, $C_v = 0$ and $C_m = 0$, $C_v = 1$.

### 6.1. *Bending moment applied to the crack faces ($C_m = 1$, $C_v = 0$)*

We first consider the following function in (75)

$$f_m(t) = t^{n_m} e^{-t}.$$

By applying the Fourier transform we obtain

$$\bar{M}_0^-(s) = \frac{\zeta^{n_m+1}\Gamma(n_m+1)}{(\zeta + \mathrm{i}s)^{n_m+1}}, \tag{78}$$

while the Mellin transform lends

$$\tilde{M}_0(s) = \int_0^\infty r^{s+1}\zeta^{n_m+1} r^{n_m} e^{-\zeta r}\mathrm{d}r = \frac{1}{\zeta^{s+1}}\Gamma(s+n_m+2). \tag{79}$$

Note that $\bar{M}_0(0) = \tilde{M}_0(-1) = \Gamma(n_m+1) \neq 0$ independent of $\zeta$. This behavior warrants that the displacement $w_0^B(x_1)$ in the free plate grows linearly to infinity along the crack line, i.e. as $x_1 \to -\infty$. After the transformations of Eqs.(54,61), one finds

$$\hat{M}_* = \frac{\zeta^{n_m+1}\Gamma(n_m+1)}{\beta_+(s)}\left(\frac{1}{(\zeta+is)^{n_m+1}} - \frac{1}{(1-\mathrm{i}s)^{\xi_M}\zeta^{n_m+1}} + \mathrm{i}\frac{s(\zeta\xi_M + n_m + 1)}{(1-\mathrm{i}s)^{\xi_M}\zeta^{n_m+2}}\right).$$

Hereinafter, for the numerics, we take

$$\nu = 0.25, \quad n_m = 4, \quad n_v = 3, \quad \xi_M = \xi_v = 7. \tag{80}$$

Owing to the absence of the sharing force, the second component of the vector from the right-hand side of the system of integral equations (72), namely $g_2(\xi)$, equals zero, while the first component, $g_1(\xi)$, can be computed in closed form, as presented in Sec.Appendix B.1. However, it was not possible to obtain an analytical representation for the kernel $\mathbf{K}(\xi)$, which is therefore computed numerically. As discussed in Section 5, we first compute the solution on the negative $\xi$-axis and then reconstruct it on the positive axis. Since the system is well defined and the projection methods converge [26], we reduce the infinite domain of integration to a finite one through controlling the behaviour of the solution at infinity. Computations are carried out on a finite grid of points whose density guarantees that the relative error is of the order of $10^{-4}$.

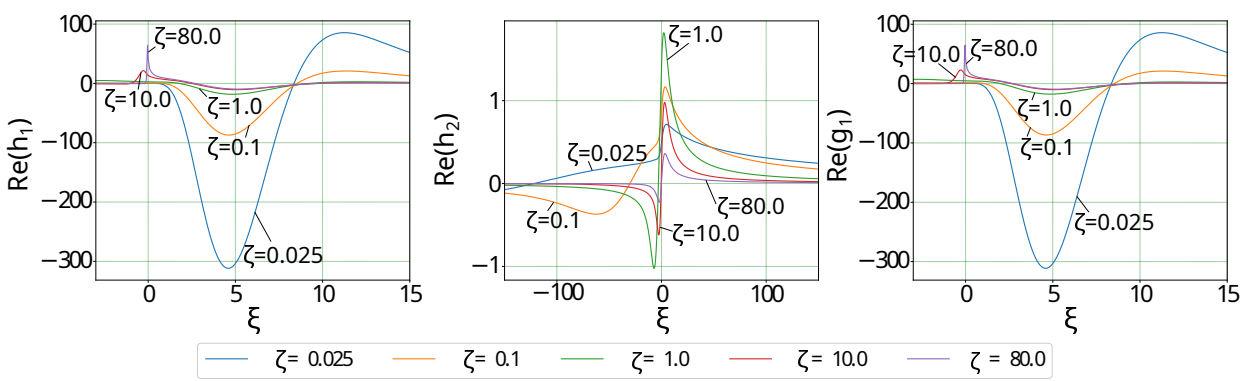


Figure 4: Numerical solution of the system of integral equations (72), in the absence of shearing force, for different values of the Winkler parameter $k = k_0\zeta^{-4}$ (compare (76)). It appears that the fisrt solution component, $h_1$, is very close to the right hand side already, while the contribution from $h_2$ is negligible.

Figure 4 shows the real part of the components in the unknown vector $\boldsymbol{h}(\xi)$ as well as the nonzero right-hand side $g_1(\xi)$ for the system of the integral equations (72). Interestingly, the first component $h_1(\xi)$ is very similar to the right-hand side $g_1(\xi)$, while the second component $h_2(\xi)$ is 2 order of magnitude smaller. This means that, within this loading, the system is almost symmetric and the numerical system diagonal. Clearly, results depend significantly on the Winkler parameter, especially near the crack-tip.

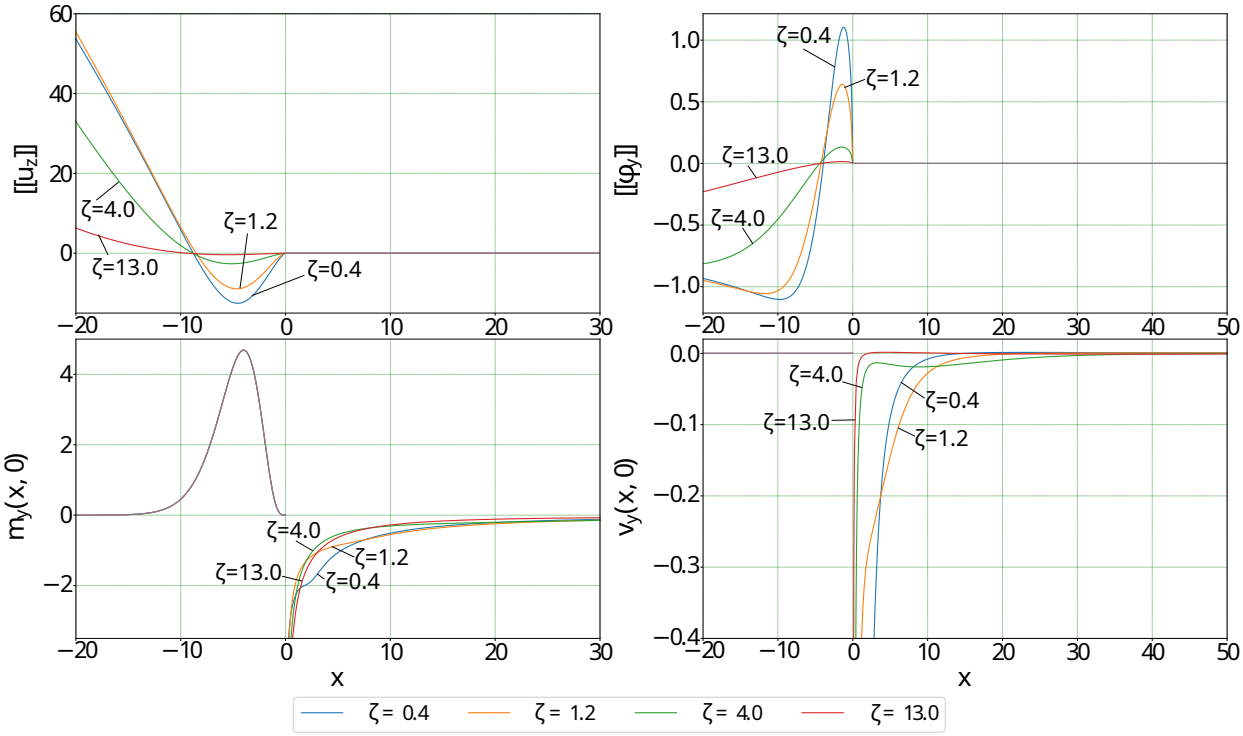


Figure 5: Jump of the displacement and rotation, bending moment and shearing force along the crack line $y = 0$ where a distribution of bending moment is applied, in the absence of shearing force, i.e. $V_0 \equiv 0$. The dimensional coordinate $x$ is used as the abscissa to bring about the role of the foundation through $\zeta$.

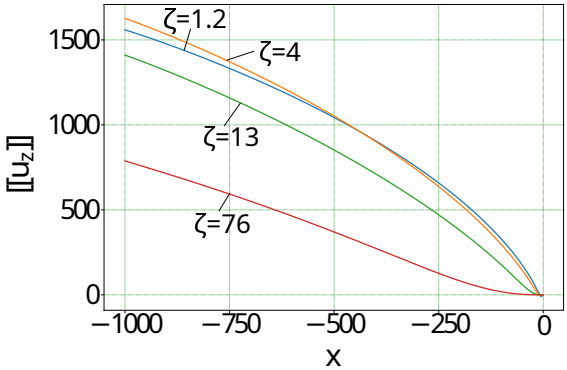


Figure 6: Far-field behavior of the jump of the displacement along the crack surfaces for the case of bending moment, i.e. $V_0 \equiv 0$.

Figure 5 illustrates the mechanical unknowns over the line $y = 0$ (that is along the crack surfaces and at the interface between the supported and the unsupported plate). It is emphasized that the jump of the displacement and slope is identically zero beyond the crack-tip ($x > 0$), while the bending moment and shearing force correspond to the applied load on the crack line ($x < 0$).

To highlight the behaviour of the solution in the far-field, Figure 6 presents the jump of the displacement on a wider interval. Here, we observe a linear growth of the displacement at infinity (compare (20)) for large value of $\zeta$ (small $k$). On the other hand, for small values of $\zeta$, square root growth represents the dominant asymptotics, that is related to the skew-symmetric part of the solution. This is in the agreement with the analysis provided in Appendix A (see Table A.1) and is a direct consequence of the condition $\tilde{M}_0(-1) \neq 0$.

Finally, Figure 7 shows the normalised SIFs as functions of the Winkler parameter $\zeta$, as computed

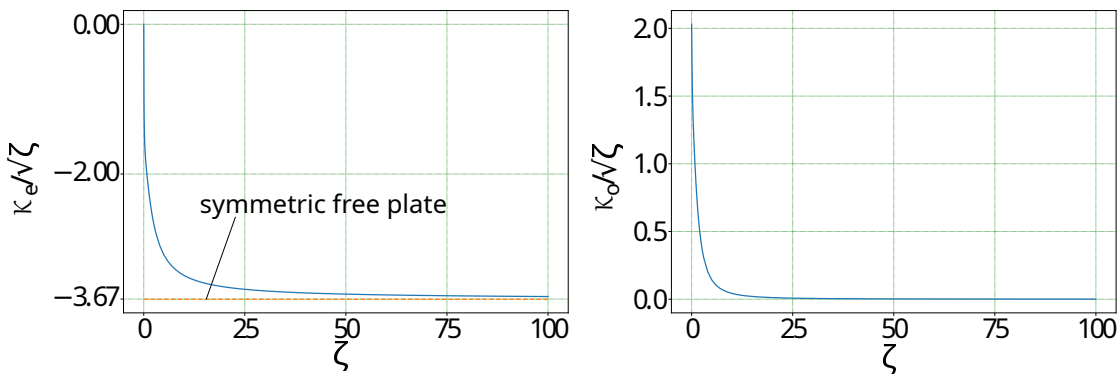


Figure 7: Normalised stress intensity factors $\zeta^{-1/2}\mathcal{K}_e(\zeta)$ and $\zeta^{-1/2}\mathcal{K}_o(\zeta)$ (compare (77)) as functions of the auxiliary parameter $\zeta$ representing changes in the Winkler parameter $k$ (see (76)): Case of applied bending moment, i.e. $V_0 \equiv 0$. The horizontal dashed line corresponds to $\zeta^{-1/2}\mathcal{K}_e$ for a free plate under symmetric conditions, see (Appendix A.9).

through the relationships (73). In particular, the limiting value of $\mathcal{K}_e$ as $\zeta \to \infty$ matches the corresponding SIF obtained setting $\nu = 0.25$ in (Appendix A.9), namely $\mathcal{K}_e\zeta^{-1/2} = -3.67085$. This appears in the Fig.7 as a horizontal asymptote. A curve fitting by the Least SQuare (LSQ) method for $\mathcal{K}_e(\zeta)\zeta^{-1/2}$ on the interval $\zeta = [65, 100]$ is given by $\mathcal{K}_o(\zeta)\zeta^{-1/2} \approx -3.668977 + 3.237402\zeta^{-1}$ as $\zeta \to \infty$, with relative error of $5.1e-04$, that is consistent with the accuracy achieved when computing the solution of the system of the integral equations.

### *6.2. Shearing force applied to the crack faces ($C_m = 0$, $C_v = 1$)*

In this case, we take $g_1 \equiv 0$ and $g_2(x) = \mathrm{i}\mathcal{F}^{-1}[\hat{V}_*(s)](x)$ as the right hand side of the system of integral equations (72). Consequently, it is

$$\bar{V}_0^-(s) = \mathrm{i}s\bar{M}_0^-(s),$$

where the function $\bar{M}_0(s)$ is defined in (78). It is easy to see that the condition $\bar{V}_0^-(0) = 0$ is satisfied automatically. The original function (after normalisation) takes the form

$$V_0(x_1) = \zeta^{n_v+1}(\zeta x_1 + n_v)(-x_1)^{n_v-1}e^{\zeta x_1}. \tag{81}$$

and its Mellin transform is

$$\tilde{V}_0^-(s) = -\frac{2+s}{\zeta^{s+1}}\Gamma(n_v + s + 2). \tag{82}$$

Hereinafter, we assume $\xi_v = 6$.

The counterparts of Figures 4–7 are presented in Figures 8–11, this time for shearing force, i.e. $M_0 \equiv 0$. In particular, Figure 8 reveals that $h_2(\xi)$ is really the dominating component of the solution, with a small contribution from $h_1(\xi)$, which fact suggests that the loading condition is close to skew-symmetry.

Figure 9 presents the mechanical unknowns for the case when a shearing force is applied. Once again we see that no jump of displacement and slope occurs beyond the crack-tip ($x > 0$), while the applied loading appears along the crack faces ($x < 0$).

To highlight the behaviour of the solution in the far field, e.g. as $x \to -\infty$, Figure 10 presents the jump of the displacement and of the slope on a wide interval. Here, we observe square root growth of the displacement at infinity (compare (20)) for large $\zeta$ (small $k$). On the other hand, for small $\zeta$ (large $k$), the displacement tends to the symmetric part of the solution and grows linearly. This again is in the agreement with the limiting analysis provided in Appendix A (see Table A.1) and is a direct consequence that the condition $\tilde{V}_0(-1) \neq 0$.

As it can be seen in Figure 11, the normalised SIF $\mathcal{K}_o\zeta^{-1/2}$ asymptotes, as $\zeta \to \infty$, to the limiting case of a free plate under skew-symmetric conditions, given in (Appendix A.6) (see Appendix A). The corresponding horizontal asymptote is drawn in the picture. Comparing this limiting value, $\mathcal{K}_o\zeta^{-1/2} = 0.831818$, with the approximated SIF computed from the solution of the system of integral equations provides the relative error of the order of $3.6 \cdot 10^{-4}$, that again is consistent with the accuracy of the computations.

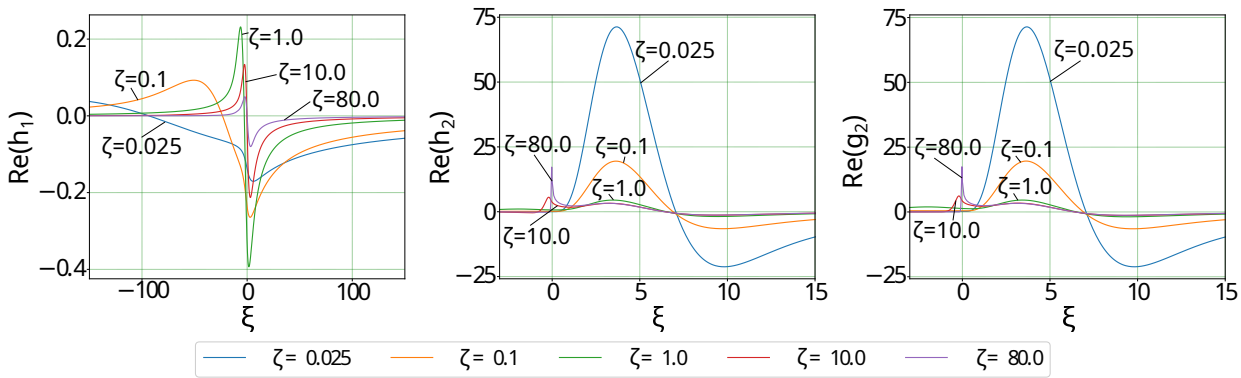


Figure 8: Numerical solution of the system of the integral equations (72) in case of applied shear force for various values of the Winkler parameter $k = k_0\zeta^{-4}$ (compare (76)). The first two graphs correspond to the two components of the solution, while the third one represents the nonzero component at the right hand side.

## 7. Conclusions

In this paper, we consider the Linear Elastic Fracture Mechanics (LEFM) problem of a thin Kirchhoff plate partially supported by a Winkler foundation, in an attempt to incorporate the role of the support in any model related to sheet cutting. Indeed, almost any (possibly nonlinear) thermo-mechanical dissipative model of cutting, at some stage, takes into consideration the LEFM stress intensity factors (SIFs). In fact, our deepest motivation lies in the observation that providing good mechanical constraining conditions is crucial for any quality cutting process. The Kirchhoff plate is endowed with a semi-infinite rectilinear crack that sits right at the boundary of the supported zone. As a result, the problem is no longer symmetric even locally, in the neighborhood of the crack-tip. The problem is first formulated in terms of a pair of coupled functional equations of the Wiener-Hopf type, whose kernel cannot be factored in general. To circumvent this shortcoming, the problem is then recast in terms of a pair of integral equations on a half-domain, which are then easily solved numerically. However, to guarantee that the numerical solution is meaningful, the problem structure is manipulated and regularized, taking advantage of the features of the mechanical setup, mostly the global equilibrium conditions in the free (unsupported) plate.

The resulting numerical system is very stable and may be efficiently computed. The numerical solution reveals that the supporting condition is very relevant in determining (a) the fields in the neighborhood of the crack-tip and (b) their asymptotic value in far-field on the crack line. Indeed, while the observation (a) is consistent with the intuition and with the fact that stable cutting requires solid support, finding (b) is somewhat surprising because it reveals that little support imperfections may be amplified in the far-field behaviour of the free plate. In fact, we show how the loading properties determine the far-field behaviour. Besides, we show that, for the limiting situation of an exceedingly stiff support and in dependence of the applied loading, SIFs converge to the case of a free plate in either symmetric or skew-symmetric deformation, or, in general, to a linear combination thereof.

Contrarily to intuition, in neither case the situation of a clamped plate is retrieved, because it possesses a different decay rate in the neighborhood of the crack tip. In general, we find that both symmetric and skew-symmetric SIFs appear simultaneously, which depend on the support stiffness in opposing fashion, namely one increases while the other decreases. As a result, although no optimal support stiffness may be envisaged, it is deduced that the role of the support is to couple the symmetric and the skew-symmetric part of the solution. Therefore, the nature of the support affects the failure mode in a fundamental manner, and it is capable of shifting failure from mode II (bending) to mode III (shear). This observation may produce far reaching consequences, once it is associated with the fact that, in general, materials behave in a very different manner when subjected to different failure modes (e.g. in shear or bending).

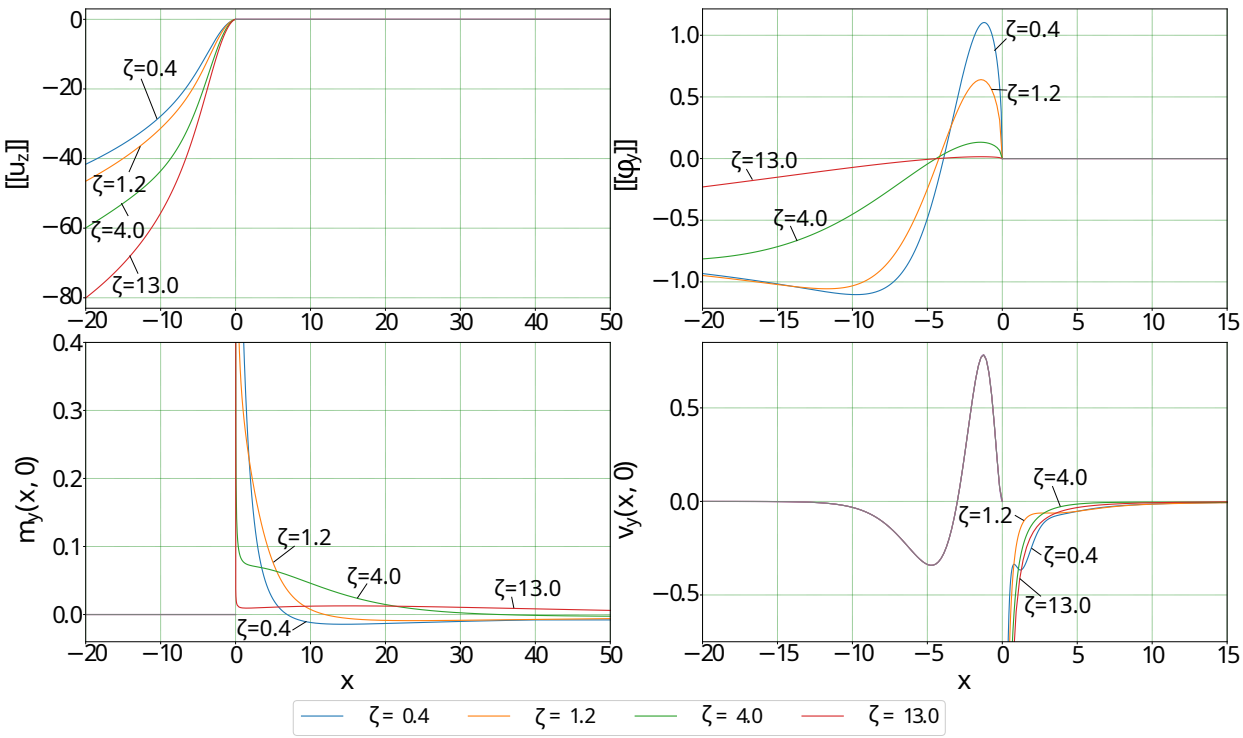


Figure 9: Jump of the displacements and of the rotations, bending moment and shearing force on the line $x_2 = 0$ for the case of applied shearing force ($M_0 \equiv 0$).


## Acknowledgments

Authors gratefully acknowledge funding from the European Union's Horizon 2020 MSCA-RISE-2020, Research and Innovation Staff Exchange, under the H2020-EU.1.3. - EXCELLENT SCIENCE - Marie Skłodowska-Curie Actions Main Programme, grant agreement No 101008140, EffectFact. GM is grateful for a three month visiting position at the University of Modena and Reggio Emilia, under the long-term visiting programme, in 2022. AN acknowledges support from the National Group of Mathematical Physics (GNFM), within the Institute of Higher Mathematics (INDAM). AN also gratefully mentions support from Mathematics for Industry 4.0 (Math4I4), under the PRIN scheme.


## Declaration of generative AI in scientific writing

Authors have not taken advantage of AI in their scientific writing

## Appendix A. Limiting problems

*Exceedingly weak foundation*

When the stiffness of the support is exceedingly week ($k \to 0$), the corresponding solution for a free plate loaded along the crack surfaces can be found in closed form and it will be a combination of two fundamental solutions, symmetric or skew-symmetric, in dependence of the prescribed loading. On the other hand, when the stiffness of the foundation becomes infinite $k \to \infty$ ($\varpi \to 0$), the plate becomes fixed on the crack line beyond the crack tip. Again, the solution is obtained by combining the symmetric and skew-symmetric fundamental loading conditions. In either case, solutions may be readily found in terms of Mellin transforms

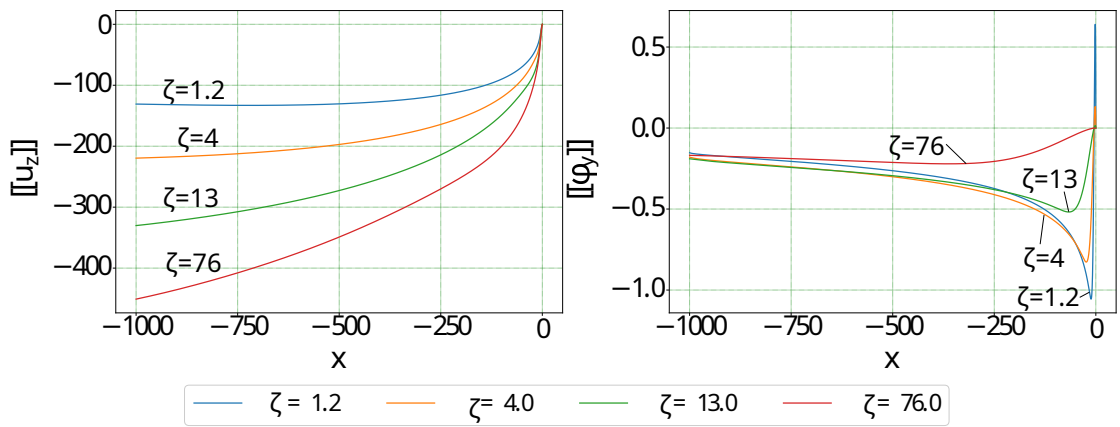


Figure 10: Jumps of the displacement and of the slope across the crack line plotted on wider range to capture the far-field asymptotics, for the case of $M_0 \equiv 0$.

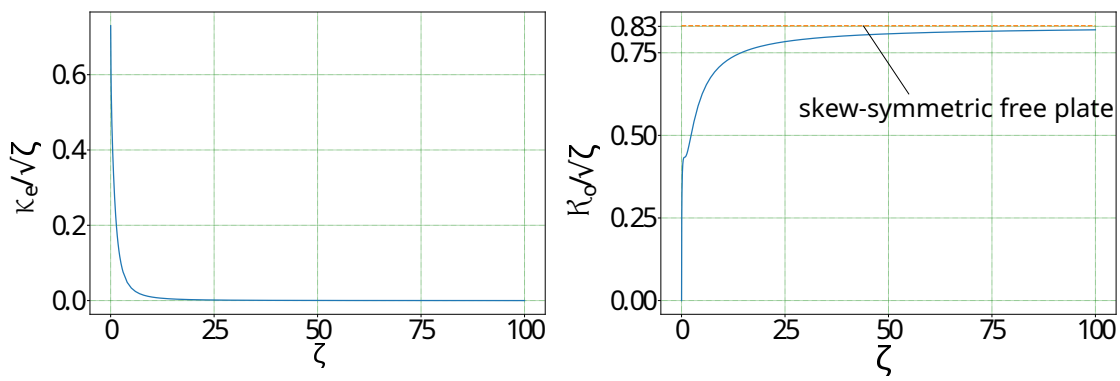


Figure 11: Normalised stress intensity factors $\zeta^{-1/2}\mathcal{K}_e(\zeta)$ and $\zeta^{-1/2}\mathcal{K}_o(\zeta)$ (compare (77)) as functions of the auxiliary parameter $\zeta$ representing changes in the Winkler parameter $k$ (see (76)): Case of applied shearing force, i.e. $M_0 \equiv 0$. Clearly, the limit of an exceedingly stiff foundation lends the SIF for a skew-symmetric free plate

(hereinafter denoted by an overtilde),

$$\tilde{w}_0^-(s) = \int_0^\infty r^{s-1} w(r,-\pi)\mathrm{d}r, \qquad \tilde{\phi}_0^-(s) = \int_0^\infty r^{s} \phi(r,-\pi)\mathrm{d}r, \tag{Appendix A.1a}$$

$$\tilde{m}_0^-(s) = \int_0^\infty r^{s+1} m(r,-\pi)\mathrm{d}r, \qquad \tilde{v}_0^-(s) = \int_0^\infty r^{s+2} v(r,-\pi)\mathrm{d}r, \tag{Appendix A.1b}$$

suitably defined to have the same strip of analyticity for all functions. The inverse of Mellin is accordingly defined as

$$w(r,-\pi) = \frac{1}{2\pi\mathrm{i}}\int_{c-\mathrm{i}\infty}^{c+\mathrm{i}\infty} r^{-s}\tilde{w}_0^-(s)\mathrm{d}s, \qquad \phi(r,-\pi) = \frac{1}{2\pi\mathrm{i}}\int_{c-\mathrm{i}\infty}^{c+\mathrm{i}\infty} r^{-s-1}\tilde{\phi}_0^-(s)\mathrm{d}s, \tag{Appendix A.2a}$$

$$m(r,-\pi) = \frac{1}{2\pi\mathrm{i}}\int_{c-\mathrm{i}\infty}^{c+\mathrm{i}\infty} r^{-s-2}\tilde{m}_0^-(s)\mathrm{d}s, \qquad v(r,-\pi) = \frac{1}{2\pi\mathrm{i}}\int_{c-\mathrm{i}\infty}^{c+\mathrm{i}\infty} r^{-s-3}\tilde{v}_0^-(s)\mathrm{d}s. \tag{Appendix A.2b}$$

We look for solutions which abide by the zero asymptotics (14), whence

$$-\tfrac{3}{2} < \Re(s) < \Re(s_*). \tag{Appendix A.3}$$

*Skew-symmetric cracked free plate*

We now consider a skew-symmetric problem along the crack line for a free plate, whence $w_0^+ = m_0^+ \equiv 0$. This solution is given by

$$\tilde{w}_0^-(s) = \frac{-(1+\nu)}{(3+\nu)(1-\nu)s(s+1)}\tilde{M}_0(s) + \frac{2\tan(\pi s)}{(3+\nu)(1-\nu)s(s+1)(s+2)}\tilde{V}_0(s), \qquad \text{(Appendix A.4)}$$

$$\tilde{\phi}_0^-(s) = \frac{-2\cot(\pi s)}{(3+\nu)(1-\nu)(s+1)}\tilde{M}_0(s) + \frac{(1+\nu)}{(3+\nu)(1-\nu)(s+1)(s+2)}\tilde{V}_0(s). \qquad \text{(Appendix A.5)}$$

For $\tilde{V}_0(s) \equiv 0$, if we have the balance condition $\tilde{M}_0(-1) = 0$ due to symmetry, then $\Re(s) < 0$, and the behaviour at infinity of $w_0^-(r)$ is $O(1)$. Similarly, we have $\phi_0^-(r) = O(1)$ at infinity. Conversely, assuming $\tilde{M}_0(-1) \neq 0$, we have $\Re(s) < -1$ and $w_0^-(r) = O(r)$ and $\phi_0^-(r) = O(\ln(r))$ at infinity. Analysing behaviour of the solution near the point $s = -3/2$ we conclude that in this case both SIFs are equal to zero:

$$\mathcal{K}_o = \mathcal{K}_e = 0.$$

For $\tilde{M}_0(s) \equiv 0$, we have $-\frac{3}{2} < \Re(s) < -\frac{1}{2}$, and the behaviour at infinity of $w_0^-(r)$ is $O(r^{1/2})$. Conversely, for $\tilde{\phi}_0^-(s)$, it is $\Re(s) < +\infty$ assuming the skew-symmetric equilibrium condition $\tilde{V}_0(-1) = 0$, whence $\phi_0^-(r)$ behaves like $V_0(r)$ at infinity. If, instead, $\tilde{V}_0(-1) \neq 0$, we have $\phi_0^-(r) = O(1)$ at infinity.

Finally, computing the residue of $\tilde{w}(s,\theta)$ at $s = -3/2$, we find

$$w(r,\theta) = \mathcal{K}_o w_o(\theta) r^{3/2} + O(r), \quad \text{as } r \to 0,$$

which matches the asymptotic analysis (14) and provides the displacement intensity factor

$$\mathcal{K}_o = -\mathrm{i}\frac{4(3\nu+5)}{3(\nu+3)(1-\nu)}\tilde{V}_0(-3/2), \quad \mathcal{K}_e = 0. \qquad \text{(Appendix A.6)}$$

*Symmetric cracked free plate*

The symmetric solution whereby $\phi_0^+ = v_0^+ = 0$ lends

$$\tilde{w}_0^-(s) = \frac{(1+\nu)}{(3+\nu)(1-\nu)s(s+1)}\tilde{M}_0(s) - \frac{2\cot(\pi s)}{(3+\nu)(1-\nu)s(s+1)(s+2)}\tilde{V}_0(s), \qquad \text{(Appendix A.7)}$$

$$\tilde{\phi}_0^-(s) = \frac{2\tan(\pi s)}{(3+\nu)(1-\nu)(s+1)}\tilde{M}_0(s) + \frac{(1+\nu))}{(3+\nu))(1-\nu)(s+1)(s+2)}\tilde{V}_0(s). \qquad \text{(Appendix A.8)}$$

Again, we first consider the case $\tilde{V}_0(s) \equiv 0$ and observe that, for $w_0^-$, we find no poles assuming the equilibrium condition $\tilde{M}_0(-1) = 0$ and it follows that $w_0^-(r)$ behaves just like $M_0(r)$ does as $r$ tends to infinity. Conversely, assuming $\tilde{M}_0(-1) \neq 0$, we have $\Re(s) < -1$ and $w_0^-(r) = O(r)$ at infinity. For $\phi_0^-(r)$ we have $\Re(s) < -1/2$ and $\phi_0^-(r) = O(r^{-1/2})$ at infinity. The residue of $w$ at $s = -3/2$ lends

$$\mathcal{K}_e = -2\mathrm{i}\frac{\nu+7}{3(1-\nu)(\nu+3)}\tilde{M}_0(-3/2), \quad \mathcal{K}_o = 0. \qquad \text{(Appendix A.9)}$$

In case $\tilde{M}_0(s) \equiv 0$, we have $\Re(s) < -1$ and $w_0^-(r) = O(\ln r)$ as $r$ goes to infinity. If $\tilde{V}_0(-1) = 0$, $\phi_0^-(r)$ behaves like $V_0(r)$ at infinity, otherwise $\phi_0^-(r) = O(1)$. In this case both SIFs are zeros.

The following table collects information on the behaviour of all possible solutions at infinity.

*Half-plate clamped and cracked along the boundary*

We consider an infinite half-plate, with a rectilinear boundary at $x_2 = 0$. The plate is clamped along this boundary for $x_1 > 0$, and it is cracked for $x_1 < 0$. Demanding $w = \phi = 0$ for $x_1 > 0$, one gets

$$\tilde{w}_0^-(s) = \frac{2(1+\nu)\tilde{M}_0\sin^2(\pi s)}{s(s+1)\Delta_{cl}(s)} + \frac{2\tilde{V}_0\sin(2\pi s)}{s(s+1)(s+2)\Delta_{cl}(s)}, \qquad \text{(Appendix A.10)}$$

$$\tilde{\phi}_0^-(s) = \frac{2\tilde{M}_0\sin(2\pi s)}{(s+1)\Delta_{cl}(s)} - \frac{2(1+\nu)\tilde{V}_0\sin^2(\pi s)}{(s+1)(s+2)\Delta_{cl}(s)}, \qquad \text{(Appendix A.11)}$$

| | | |
|---|---|---|
| skew-symmetric | $\tilde{V}_0(s) \equiv 0$ | $\tilde{M}_0(s) \equiv 0$ |
| $w_0^-(r)$ | $O(1)$ if $\tilde{M}_0(-1) = 0$, $O(r)$ otherwise | $O(r^{-1/2})$ if $\tilde{V}_0(-1/2) = 0$, $O(\sqrt{r})$ otherwise |
| $\phi_0^-(r)$ | $O(1)$ if $\tilde{M}_0(-1) = 0$, $O(\ln(r))$ otherwise | $V_0(r)$ if $\tilde{V}_0(-1) = 0$, $O(1)$ otherwise |
| symmetric | $\tilde{V}_0(s) \equiv 0$ | $\tilde{M}_0(s) \equiv 0$ |
| $w_0^-(r)$ | $O(1)$ if $\tilde{M}_0(-1) = 0$, $O(r)$ otherwise | $O(1)$ if $\tilde{V}_0(-1) = 0$, $O(\ln r)$ otherwise |
| $\phi_0^-(r)$ | $O(1/\sqrt{r})$ | $V_0(r)$ if $\tilde{V}_0(-1) = 0$, $O(1)$ otherwise |

Table A.1: Behaviour of the solutions of the limiting problems as $r \to \infty$

where

$$\Delta_{cl}(s) = 4 + (3-\nu)^2 + (1-\nu)(3+\nu)\cos(2\pi s).$$

The first pole of this solution is located at $s = -3/2 \pm \mathrm{i}\varepsilon$, where

$$\varepsilon = \frac{1}{2\pi}\cosh^{-1}\left(\frac{4+(3-\nu)^2}{(1-\nu)(3+\nu)}\right) > 0.$$

Thus, the singularity in the displacement takes the form

$$w(r,\theta) = O(r^{3/2\mp\mathrm{i}\varepsilon}), \qquad \text{as } r \to 0,$$

which does not match the singularity of the problem in the presence of a foundation, no matter how stiff. Interestingly, a recent paper [11] has been devoted to analysis of the stress singularity for a partially clamped plate with a crack on the boundary exhibiting surface stress effects.

## Appendix B. Forcing terms in the system of integral equations

### *Appendix B.1. Bending moment*

$$g_1(x) = \mathcal{F}^{-1}[\hat{M}_*(s)](x) = \begin{cases} \frac{\zeta^{n_m+1}\sqrt{2}}{1+\mathrm{i}}(-x)^{n_m+\frac{1}{2}}e^{\zeta x}U\left(\frac{1}{2},\frac{3}{2}+n_m,-\zeta x\right), & x<0, \\ \frac{\sqrt{2}\Gamma(n_m+1)}{1+\mathrm{i}}\Bigg(\sqrt{\frac{\zeta}{\pi}}U\left(\frac{1}{2},\frac{1}{2}-n_m,\zeta x\right) - \frac{x^{\xi_M-\frac{1}{2}}}{\Gamma\left(\xi_M+\frac{1}{2}\right)}M\left(\xi_M,\xi_M+\frac{1}{2},-x\right) - \\ \qquad \frac{(2\xi_M-1)(n_m+\zeta\xi_M+1)\Gamma(\frac{1}{2}-\xi_M)}{2\pi\zeta}\cos(\pi\xi_M)x^{\xi_M-\frac{3}{2}}M\left(\xi_M,\xi_M-\frac{1}{2},-x\right)\Bigg), & x>0, \end{cases} \tag{Appendix B.1}$$

where $M(a,b,c)$ is Kummer's and $U(a,b,c)$ Tricomi's (confluent hypergeometric) function (for the definitions, see [12]).

## Appendix C. Asymptotics of the solution components in the frequency domain

### *Appendix C.1. Asymptotic behavior at $s = 0$*

#### *Appendix C.1.1. Analysis of the balance conditions*

The notation (36) is motivated by the following analysis which demonstrates that

$$A_j(0) = B_j(0) = 0.$$

Indeed, rewriting (27) through (33), we get, for the supported plate, an homogeneous systems of three linear equations in the unknowns $A_j$, namely

$$\lim_{s\to 0}\left[A_1\left(\alpha_1^2-\nu s^2\right)+A_2\left(\alpha_2^2-\nu s^2\right)\right]=0,$$

$$\lim_{s\to 0}\left[\alpha_1 A_1\left(\alpha_1^2+(\nu-2)s^2\right)+\alpha_2 A_2\left(\alpha_2^2+(\nu-2)s^2\right)\right]=0,$$

$$\lim_{s\to 0}\frac{\mathrm{d}}{\mathrm{d}s}\Big(\alpha_1 A_1\left(\alpha_1^2+(\nu-2)s^2\right)+\alpha_2 A_2\left(\alpha_2^2+(\nu-2)s^2\right)\Big)=0.$$

Recalling (30), we observe that the first pair of equations provide a regular system with determinant $\big(\alpha_2(0)-\alpha_1(0)\big)\alpha_1^2(0)\alpha_2^2(0)\neq 0$, whence $A_j(0)=0$, $(j=1,2)$. Consequently, alongside the balance conditions (27), we have

$$\bar{w}_0^A(0)=\bar{\phi}_0^A(0)=0. \tag{Appendix C.1}$$

The last equation gives immediately

$$\lim_{s\to 0}\left[\alpha_1^3(0)A_1'(s)+\alpha_2^3(0)A_2'(s)\right]=0,$$

whence, by (30),

$$A_1'(s)=\mathrm{i}A_2'(s)+O(|s|),\quad s\to 0. \tag{Appendix C.2}$$

In terms of asymptotic estimates, this gives either $(j=1,2)$

$$A_j(s)\sim a_j s^{\varpi},\quad a_1=\mathrm{i}a_2,\quad s\to 0,\quad 0<\varpi\leq 1, \tag{Appendix C.3}$$

that will be proved incorrect in Eq.(Appendix C.17), or

$$A_j(s)\sim a_j s^{\varpi_j},\quad s\to 0,\quad \varpi_j>1, \tag{Appendix C.4}$$

with $a_1$ and $a_2$ complex-valued constants. The same path of reasoning may be carried out for $B_j(s)$, but we choose to follow another approach.

*Appendix C.1.2. Connecting $B_*$, $B_2$ to the transforms $\bar{m}_0$ and $\bar{v}_0$*

Specializing (34) to the crack line and accounting for (36), one finds

$$\bar{m}_0=-(\nu-1)\beta B_*+2\beta B_2, \tag{Appendix C.5a}$$

$$\bar{v}_0=(\nu-1)s^2B_*+(\nu+1)s^2B_2, \tag{Appendix C.5b}$$

where no superscript appears at LHS in light of (25). This system of equations provides a non-singular constant-coefficient linear transformation of the functions $B_*$ and $B_2$ to $\bar{m}_0$ and $\bar{v}_0$, whence these share the same asymptotics. We may easily solve the linear system

$$\begin{bmatrix}B_*\\B_2\end{bmatrix}=\begin{bmatrix}1-\nu & 2\\ \nu-1 & 1+\nu\end{bmatrix}^{-1}\begin{bmatrix}\beta^{-1}\bar{m}_0\\ s^{-2}\bar{v}_0\end{bmatrix}=\frac{1}{4c}\begin{bmatrix}1+\nu & -2\\ 1-\nu & 1-\nu\end{bmatrix}\begin{bmatrix}\beta^{-1}\bar{m}_0\\ s^{-2}\bar{v}_0\end{bmatrix}, \tag{Appendix C.6}$$

to get

$$B_*=\frac{(1+\nu)\bar{m}_0\beta^{-1}-2\bar{v}_0s^{-2}}{(1-\nu)(3+\nu)},\quad B_2=\frac{1}{3+\nu}\Big(\bar{m}_0\beta^{-1}+\bar{v}_0s^{-2}\Big). \tag{Appendix C.7}$$

*Appendix C.1.3. Refined asymptotics at zero*

Taking advantage of the results (35), we can better determine the asymptotics of $B_*$ and $B_2$ (and likewise for $A_1, A_2$) as $s \to 0$. We begin with the transformed bending moment $\bar{m}_0(s)$. First, it follows from (21) and (16b), that $m_0^{A,B}(x_1) \in L_1(\mathbb{R})$, $x_1 m_0^{A,B}(x_1) \in L_1(\mathbb{R})$, as a result, we conclude that $\bar{m}_0(s) = \bar{m}(s,0) \in \mathbb{C}^1_{loc}$ and thus

$$\bar{m}_0(s) = \mathfrak{m}_0 + \mathfrak{m}_1 s + O(|s|^{3/2}), \quad s \to 0. \tag{Appendix C.8}$$

Similarly, it follows from (21) and (16c), that $v_0^{A,B}(x_1) \in L_1(\mathbb{R})$, $x_1 v^{A,B}(x_1) \in L_1(\mathbb{R})$ and $x_1^2 v^{A,B}(x_1) \in L_1(\mathbb{R})$, as a result, we conclude that $\bar{v}_0(s) = \bar{v}(s,0) \in \mathbb{C}^2_{loc}$ near the origin and thus

$$\bar{v}_0(s) = \mathfrak{v}_0 + \mathfrak{v}_1 s + \mathfrak{v}_2 s^2 + O(|s|^{5/2}), \quad s \to 0. \tag{Appendix C.9}$$

From the transformed balance conditions (27), it immediately follows that $\mathfrak{m}_0 = \mathfrak{v}_0 = \mathfrak{v}_1 = 0$. Besides, plugging (Appendix C.4,Appendix C.7) into (35a), one gets

$$[\![\bar{w}]\!] \sim a_1 s^{\varpi_1} + a_2 s^{\varpi_2} - \frac{1}{(1-\nu)(3+\nu)}\Big((1+\nu)\mathfrak{m}_1 \operatorname{sign} s - 2\mathfrak{v}_2\Big)\beta^{-1} + O(|s|^{-1/2}), \quad s \to 0, \tag{Appendix C.10}$$

and for this to be consistent with the first of (20) it is necessary that the $\beta^{-1}$-term drops out, i.e. $\pm(1+\nu)\mathfrak{m}_1 = 2\mathfrak{v}_2$ as $s \to \pm 0$. Similarly, using (Appendix C.4,Appendix C.7) into (35b) and recalling (30), we get

$$\begin{aligned}[\![\bar{\phi}]\!] \sim -e^{-\mathrm{i}\pi/4} a_1 s^{\varpi_1} - e^{\mathrm{i}\pi/4} a_2 s^{\varpi_2} - \frac{1}{(1-\nu)(3+\nu)}\Big((1+\nu)\mathfrak{m}_1 \operatorname{sign} s - 2\mathfrak{v}_2\Big) \\ - \frac{1}{3+\nu}\Big(\mathfrak{m}_1 \operatorname{sign} s + \mathfrak{v}_2\Big) + O(|s|^{1/2}), \quad s \to 0,\end{aligned} \tag{Appendix C.11}$$

and the constant term needs to disappear, i.e. $\pm\mathfrak{m}_1 = \mathfrak{v}_2$ as $s \to \pm 0$. As a result, one concludes that

$$\mathfrak{m}_1 = \mathfrak{v}_2 = 0. \tag{Appendix C.12}$$

Then, we can write the respective assumptions for $\bar{m}_0(s)$ and $\bar{v}_0(s)$ more accurately

$$\bar{m}_0(s) = O(|s|^{3/2}), \quad \bar{v}_0(s) = O(|s|^{5/2}), \quad s \to 0, \tag{Appendix C.13}$$

and returning back to (Appendix C.7) we conclude that

$$B_*(s), B_2(s) = O(|s|^{1/2}), \quad s \to 0. \tag{Appendix C.14}$$

With this knowledge, returning back to Eq.(35c) while substituting the asymptotics (Appendix C.4,Appendix C.14), we get

$$\bar{m}_0^A = -\mathrm{i} a_1 s^{\varpi_1} + \mathrm{i} a_2 s^{\varpi_2} = O(|s|^{3/2}), \quad s \to 0. \tag{Appendix C.15}$$

The same argument, this time applied to (35d), gives

$$\bar{v}_0^A = -e^{-\mathrm{i}3\pi/4} a_1 s^{\varpi_1} - e^{\mathrm{i}3\pi/4} a_2 s^{\varpi_2} = O(|s|^{5/2}), \quad s \to 0, \tag{Appendix C.16}$$

and the system (Appendix C.15,Appendix C.16) is consistent only if

$$\varpi_1 = \varpi_2 = \frac{3}{2}, \tag{Appendix C.17}$$

and we finally prove that the asymptotics (Appendix C.3) is incorrect. Furthermore, plugging this result into (Appendix C.16), one sees that

$$a_1 = \mathrm{i} a_2, \tag{Appendix C.18}$$

whence we obtain the leading asymptotics of $\bar{w}_0^A$ and $\bar{\phi}_0^A$ at the origin, namely

$$\bar{w}_0^A = A_1 + A_2 = (1+\mathrm{i}) a_2 s^{3/2}, \quad \bar{\phi}_0^A = -\alpha_1 A_1 - \alpha_2 A_2 = -\sqrt{2}(1+\mathrm{i}) a_2 s^{3/2}, \quad s \to 0. \tag{Appendix C.19}$$

*Appendix C.2. Asymptotic behavior at $s \to \pm\infty$*

From the Abelian theorem [22] applied to (16b), it follows

$$\bar{m}_0^+(s) = \mathfrak{m}_\infty e^{\pm \mathrm{i}\pi/4}|s|^{-1/2} + O(|s|^{-1}), \quad s \to \pm\infty, \tag{Appendix C.20}$$

where, clearly,

$$\mathfrak{m}_\infty = \frac{12\sqrt{\pi}c}{\nu+7}\mathcal{K}_e.$$

Likewise, from (10), it is

$$\bar{m}_0^-(s) \equiv \bar{M}_0^-(s) = O\left(s^{-1-\gamma_0}\right), \quad |s| \to \infty,\ \Im(s) < 0, \tag{Appendix C.21}$$

that, recalling $\gamma_0 > \frac{1}{2}$, decays faster than (Appendix C.20). Thus, summing (Appendix C.20) and (Appendix C.21) together, we have

$$\bar{m}_0(s) = b_1|s|^{-1/2} = \mathfrak{m}_\infty e^{\pm \mathrm{i}\pi/4}|s|^{-1/2} + O(|s|^{-1}), \quad s \to \pm\infty. \tag{Appendix C.22}$$

In similar fashion, it follows from (16c) and the Abelian theorem that

$$\bar{v}_0^+(s) = \mathfrak{v}_\infty e^{\mp \mathrm{i}\pi/4}|s|^{1/2} + O(1), \quad s \to \pm\infty, \tag{Appendix C.23}$$

with

$$\mathfrak{v}_\infty = \frac{12\sqrt{\pi}c}{3\nu+5}\mathcal{K}_o.$$

Again, the applied shearing force decays faster because it was assumed $\gamma_0 > \frac{1}{2}$

$$\bar{v}_0^-(s) = \bar{V}_0^-(s) = O(s^{-\gamma_0}), \quad |s| \to \infty,\ \Im(s) < 0, \tag{Appendix C.24}$$

whence, summing, one gets

$$\bar{v}_0(s) = b_2|s|^{\frac{1}{2}} = \mathfrak{v}_\infty e^{\mp \mathrm{i}\pi/4}|s|^{\frac{1}{2}} + O(1), \quad s \to \pm\infty, \tag{Appendix C.25}$$

whose diverging character denotes that this is a Fourier transform in the sense of distributions.

Substituting the asymptotics (Appendix C.22) and (Appendix C.25) into (33b) and (33c), respectively, we get a linear system for the asymptotics of $A_{1,2}(s)$, namely

$$\begin{cases} (\alpha_1^2 - \nu s^2)A_1 + (\alpha_2^2 - \nu s^2)A_2 = b_1|s|^{-1/2}, \\ -\alpha_1(\alpha_1^2 + (\nu-2)s^2)A_1 - \alpha_2(\alpha_2^2 + (\nu-2)s^2)A_2 = b_2|s|^{1/2}, \end{cases} \quad s \to \pm\infty. \tag{Appendix C.26}$$

Lets write this system in the form

$$\mathbf{M}\boldsymbol{a} = \boldsymbol{b}, \quad s \to \pm\infty, \tag{Appendix C.27}$$

where

$$\mathbf{M} = \begin{bmatrix} \alpha_1^2 - \nu s^2 & \alpha_2^2 - \nu s^2 \\ -\alpha_1\left(\alpha_1^2 + (\nu-2)s^2\right) & -\alpha_2\left(\alpha_2^2 + (\nu-2)s^2\right) \end{bmatrix}, \tag{Appendix C.28}$$

and

$$\boldsymbol{b} \sim \left[b_1|s|^{-1/2}, b_2|s|^{1/2}\right], \quad s \to \pm\infty, \tag{Appendix C.29}$$

This system is nonsingular (at least at infinity), for we have

$$\det \mathbf{M} = -4\mathrm{i}c|s|^3 + O(|s|^{-1}), \quad s \to \pm\infty. \tag{Appendix C.30}$$

Hence, it can be solved giving

$$\begin{cases} A_1 = \frac{\mathrm{i}(b_1-b_2)}{\nu+3}|s|^{-1/2} + \frac{b_1(\nu+1)+2b_2}{2(1-\nu)(\nu+3)}|s|^{-5/2} + o(|s|^{-5/2}), \\ A_2 = -\frac{\mathrm{i}(b_1-b_2)}{\nu+3}|s|^{-1/2} + \frac{b_1(\nu+1)+2b_2}{2(1-\nu)(\nu+3)}|s|^{-5/2} + o(|s|^{-5/2}), \end{cases} \quad s \to \pm\infty. \tag{Appendix C.31}$$

By substituting this expansion into the general solution (29) for the supported plate, we obtain, to leading order,

$$\bar{w}_0^A = A_1 + A_2 = \frac{b_1(\nu+1)+2b_2}{(1-\nu)(\nu+3)}|s|^{-5/2}, \quad s \to \pm\infty,$$

whence

$$\bar{w}_0^A = 3\sqrt{\pi}\left(e^{\pm \mathrm{i}\pi/4}\mathcal{K}_e\frac{\nu+1}{\nu+7} + e^{\mp \mathrm{i}\pi/4}\mathcal{K}_o\frac{2}{3\nu+5}\right)|s|^{-5/2}, \quad s \to \pm\infty. \qquad \text{(Appendix C.32)}$$

Similarly, substituting (Appendix C.31) into (33a), we get

$$\bar{\phi}_0^A = -\alpha_1 A_1 - \alpha_2 A_2 = -\frac{b_2(\nu+1)+2b_1}{(1-\nu)(\nu+3)}|s|^{-3/2},$$

thus, to leading order,

$$\bar{\phi}_0^A = -3\sqrt{\pi}e^{\pm \mathrm{i}\pi/4}\left(\frac{2}{\nu+7}\mathcal{K}_e \pm \mathrm{i}\frac{\nu+1}{3\nu+5}\mathcal{K}_o\right)|s|^{-3/2}, \quad s \to \pm\infty. \qquad \text{(Appendix C.33)}$$

*Appendix C.3. Asymptotics of the half-transforms $\bar{w}^\pm$, $\bar{\phi}^\pm$, $\bar{m}^\pm$, $\bar{v}^\pm$*

In the previous Sections, we have obtained the asymptotics of the full range Fourier transforms, both as $s \to 0$ and as $s \to \pm\infty$, see Table C.2. Moving from these, we here deduce, the corresponding behaviour of

| | $s \to 0$ | $\lvert s\rvert \to \infty$ |
|---|---|---|
| $\bar{w}_0^A$ | $s^{3/2}$ | $s^{-5/2}$ |
| $\bar{\phi}_0^A$ | $s^{3/2}$ | $s^{-3/2}$ |
| $\bar{m}_0 = \bar{m}^+$ | $s^{3/2}$ | $s^{-1/2}$ |
| $\bar{v}_0 = \bar{v}^+$ | $s^{5/2}$ | $s^{1/2}$ |
| $[\![\bar{w}]\!] = [\![\bar{w}^-]\!]$ | $s^{-1/2}$ | $s^{-5/2}$ |
| $[\![\bar{\phi}]\!] = [\![\bar{\phi}^-]\!]$ | $s^{1/2}$ | $s^{-3/2}$ |

Table C.2: Asymptotics of the full range Fourier transforms

the half-transforms. From the Taylor expansion of (23) as $s \to 0$, we write

$$\bar{\phi}_0^+(s) = \int_0^\infty \phi_0(x)\mathrm{d}x + O(s^{1/2}), \quad \bar{\phi}_0^{B-}(s) = \int_{-\infty}^0 \phi_0^B(x)\mathrm{d}x + O(s^{1/2}), \qquad s \to 0, \quad \text{(Appendix C.34a)}$$

$$\bar{m}_0^+(s) = \int_0^{+\infty} m_0(x)\mathrm{d}x + \mathrm{i}s\int_0^{+\infty} x m_0(x)\mathrm{d}x + O(s^{3/2}), \quad s \to 0, \quad \text{(Appendix C.34b)}$$

$$\bar{m}_0^-(s) = \int_{-\infty}^0 M_0(x)\mathrm{d}x + \mathrm{i}s\int_{-\infty}^0 x M_0(x)\mathrm{d}x + O(s^2), \quad s \to 0, \quad \text{(Appendix C.34c)}$$

$$\bar{v}_0^+(s) = \int_0^{+\infty} v_0(x)\mathrm{d}x + \mathrm{i}s\int_0^{+\infty} x v_0(x)\mathrm{d}x - \tfrac{1}{2}s^2\int_0^{+\infty} x^2 v_0(x)\mathrm{d}x + O(s^{5/2}), \quad s \to 0, \quad \text{(Appendix C.34d)}$$

$$\bar{v}_0^- = \int_{-\infty}^0 V_0(x)\mathrm{d}x + \mathrm{i}s\int_{-\infty}^0 x V_0(x)\mathrm{d}x - \tfrac{1}{2}s^2\int_{-\infty}^0 x^2 V_0(x)\mathrm{d}x + O(s^3), \quad s \to 0. \quad \text{(Appendix C.34e)}$$

Accounting for (Appendix C.13), we deduce the asymptotics

$$\bar{m}_0^+(s) = -\bar{M}_0^-(0) - s\frac{\mathrm{d}\bar{M}_0^-}{\mathrm{d}s}(0) + O(s^{3/2}), \quad s \to 0, \qquad \text{(Appendix C.35a)}$$

$$\bar{v}_0^+(s) = -\bar{V}_0^-(0) - s\frac{\mathrm{d}\bar{V}_0^-}{\mathrm{d}s}(0) - \tfrac{1}{2}s^2\frac{\mathrm{d}^2\bar{V}_0^-}{\mathrm{d}s^2}(0) + O(s^{5/2}), \quad s \to 0. \qquad \text{(Appendix C.35b)}$$

Also, from (Appendix C.10) and (Appendix C.11) we have

$$[\![\bar{w}]\!] = O(s^{-1/2}), \quad [\![\bar{\phi}]\!] = \bar{\phi}_0^A - (\bar{\phi}_0^+ + \bar{\phi}_0^{B-}) = O(s^{1/2}), \quad s \to 0, \tag{Appendix C.36}$$

where, recalling (Appendix C.19), it is $\bar{w}_0^A = O(s^{3/2})$ and $\bar{\phi}_0^A = O(s^{3/2})$. For the last asymptotics to hold true, it is required that

$$\int_{-\infty}^{\infty} \phi_0(s)\mathrm{d}x = 0.$$

The asymptotics at infinity are compute directly taking the positive half-transform of (14,16)

$$\bar{w}_0^+(s) = \mathrm{i}W_0 s^{-1} - W_1 s^{-2} + 3\sqrt{\pi}\frac{\nu+1}{\nu+7}e^{\pm\mathrm{i}\pi/4}\mathcal{K}_e|s|^{-5/2} + O(s^{-7/2}), \qquad s \to \pm\infty, \tag{Appendix C.37a}$$

$$\bar{\phi}_0^+(s) = \mathrm{i}W_2 s^{-1} - 3\sqrt{\pi}\frac{\nu+1}{3\nu+5}e^{\mp\mathrm{i}\pi/4}\mathcal{K}_o|s|^{-3/2} + O(s^{-5/2}), \qquad s \to \pm\infty, \tag{Appendix C.37b}$$

$$\bar{m}_0^+(s) = 12c\sqrt{\pi}\frac{e^{\pm\mathrm{i}\pi/4}}{\nu+7}\mathcal{K}_e|s|^{-1/2} + O(s^{-3/2}), \qquad s \to \pm\infty, \tag{Appendix C.37c}$$

$$\bar{v}_0^+(s) = 12c\sqrt{\pi}\frac{e^{\mp\mathrm{i}\pi/4}}{3\nu+5}\mathcal{K}_o|s|^{1/2} + C_1 + O(s^{-1/2}), \qquad s \to \pm\infty. \tag{Appendix C.37d}$$

where the first two formulae are valid inasmuch as $\Im(s) > 0$ and the last only in the sense of distributions. Similarly, for the negative half transforms, we get

$$\bar{w}_0^{B-}(s) = -\mathrm{i}W_0 s^{-1} + W_1 s^{-2} - 6\sqrt{\pi}\frac{e^{\mp\mathrm{i}\pi/4}}{3\nu+5}\mathcal{K}_o|s|^{-5/2} + O(s|^{-7/2}), \qquad s \to \pm\infty, \tag{Appendix C.38a}$$

$$\bar{\phi}_0^{B-}(s) = -\mathrm{i}W_2 s^{-1} + 6\sqrt{\pi}\frac{e^{\pm\mathrm{i}\pi/4}}{\nu+7}\mathcal{K}_e|s|^{-3/2} + O(s^{-5/2}), \qquad s \to \pm\infty, \tag{Appendix C.38b}$$

$$\bar{m}_0^-(s) = \bar{M}_0^-(s) = O(s^{-\gamma_0-1}), \quad \bar{v}_0^-(s) = \bar{V}_0^-(s) = O(s^{-\gamma_0}), \qquad s \to \infty, \tag{Appendix C.38c}$$

Accounting for (Appendix C.32,Appendix C.33), we obtain, to leading order,

$$\begin{aligned} &[\![\bar{w}]\!] = \bar{w}_0^A - (\bar{w}_0^+ + \bar{w}^{B-}) \sim 12\sqrt{\pi}\tfrac{e^{\mp\mathrm{i}\pi/4}}{5+3\nu}\mathcal{K}_o|s|^{-5/2}, \\ &[\![\bar{\phi}]\!] = \bar{\phi}_0^A - (\bar{\phi}_0^+ + \bar{\phi}^{B-}) \sim -12\sqrt{\pi}\tfrac{e^{\pm\mathrm{i}\pi/4}}{7+\nu}\mathcal{K}_e|s|^{-3/2}, \qquad s \to \pm\infty. \\ &\bar{m}_0 \sim \mathfrak{m}_\infty e^{\pm\mathrm{i}\pi/4}\mathcal{K}_e|s|^{-1/2}, \qquad \bar{v}_0 \sim \mathfrak{v}_\infty e^{\mp\mathrm{i}\pi/4}\mathcal{K}_o|s|^{1/2}, \end{aligned} \tag{Appendix C.39}$$

## References


[1] DD Ang, ES Folias, and ML Williams. The bending stress in a cracked plate on an elastic foundation. *Journal of Applied Mechanics*, 1963.

[2] T Atkins. *The science and engineering of cutting: the mechanics and processes of separating, scratching and puncturing biomaterials, metals and non-metals.* Butterworth-Heinemann, 2009.

[3] Z-Q Cheng and JN Reddy. Green's functions for an anisotropic thin plate with a crack or an anticrack. *International journal of engineering science*, 42(3-4):271–289, 2004.

[4] K-R Deibel, C Raemy, and K Wegener. Modeling slice-push cutting forces of a sheet stack based on fracture mechanics. *Engineering Fracture Mechanics*, 124:234–247, 2014.

[5] ES Folias. On a plate supported by an elastic foundation and containing a finite crack. *International Journal of Fracture Mechanics*, 6(3):257–263, 1970.

[6] J P Gallagher. Usaf damage tolerant design handbook: guidelines for the analysis and design of damage tolerant aircraft structures. Technical report, 1984.

[7] R V Gol'dstein and R L Salganik. Brittle fracture of solids with arbitrary cracks. *International journal of Fracture*, 10:507–523, 1974.

[8] N Gorbushin, V Eremeyev, and G Mishuris. On stress singularity near the tip of a crack with surface stresses. *International Journal of Engineering Science*, 146:103183, 2020.

[9] RJ Hartranft and GC Sih. An approximate three-dimensional theory of plates with application to crack problems. *International Journal of Engineering Science*, 8(8):711–729, 1970.

[10] C-W Hsu and C Hwu. Green's functions for unsymmetric composite laminates with inclusions. *Proceedings of the Royal Society A*, 476(2233):20190437, 2020.

[11] Zhen-Liang Hu, Xue-Yang Zhang, and Xian-Fang Li. Oscillatory singularity for bending of a partially clamped nanoplate with consideration of surface effect. *Engineering Fracture Mechanics*, page 109495, 2023.

[12] I.S.Gradshtein and I.M.Ryzhik. *Tables of integrals, series and products.* Academic Press, fifth edition, 1996.

[13] VGMD Kumar, MD German, and C F Shih. Engineering approach for elastic-plastic fracture analysis. Technical report, General Electric Co., 1981.

[14] H Liebowitz and GC Sih. Mathematical theories of brittle fracture. chapter 2. ACADEMIC PRESS, INC.,, 1968.

[15] P C Miedlar, A P Berens, A Gunderson, and JP Gallagher. Analysis and support initiative for structural technology (asist) delivery order 0016: Usaf damage tolerant design handbook: guidelines for the analysis and design of damage tolerant aircraft structures. Technical report, DAYTON UNIV OH RESEARCH INST, 2002.

[16] SA Mohamed, S Bichir, MS Matbuly, and M Nassar. Analytical solution of cracked shell resting on elastic foundation. *Acta mechanica solida sinica*, 9(4):306–319, 1996.

[17] A Nobili, E Radi, and L Lanzoni. A cracked infinite kirchhoff plate supported by a two-parameter elastic foundation. *Journal of the European Ceramic Society*, 34(11):2737–2744, 2014.

[18] A Nobili, E Radi, and L Lanzoni. On the effect of the backup plate stiffness on the brittle failure of a ceramic armor. *Acta Mechanica*, 227:159–172, 2016.

[19] A Nobili, E Radi, and L Lanzoni. Flexural edge waves generated by steady-state propagation of a loaded rectilinear crack in an elastically supported thin plate. *Proceedings of the Royal Society A: Mathematical, Physical and Engineering Sciences*, 473(2204):20170265, 2017.

[20] Andrea Nobili and Valentina Volpini. Microstructured induced band pattern in love wave propagation for novel nondestructive testing (ndt) procedures. *International Journal of Engineering Science*, 168:103545, 2021.

[21] B Noble. *Methods based on the Wiener-Hopf technique for the solution of partial differential equations, International Series of Monographs on Pure and Applied Mathematics. Vol. 7.* Pergamon Press, New York, 1958.

[22] A Piccolroaz, G Mishuris, and A Movchan. Symmetric and skew-symmetric weight functions in 2d perturbation models for semi-infinite interfacial cracks. *Journal of the Mechanics and Physics of Solids*, 57:1657–1682, 2009.

[23] A Piccolroaz, D Peck, M Wrobel, and G Mishuris. Energy release rate, the crack closure integral and admissible singular fields in fracture mechanics. *International Journal of Engineering Science*, 164:103487, 2021.

[24] Y Pronina, A Maksimov, and M Kachanov. Crack approaching a domain having the same elastic properties but different fracture toughness: Crack deflection vs penetration. *International Journal of Engineering Science*, 156:103374, 2020.

[25] DV Ramsamooj. Fracture of highway and airport pavements. *Engineering Fracture Mechanics*, 44(4):609–626, 1993.

[26] S Rogosin and G Mishuris. Constructive methods for factorization of matrix-functions. *IMA Journal of Applied Mathematics*, 81:365–391, 2016.

[27] G C Sih. Bending of a cracked plate with arbitrary stress distribution across the thickness. Technical report, NASA Technical report Nr.6, 1969.

[28] G C Sih. A review of the three-dimensional stress problem for a cracked plate. *International Journal of Fracture Mechanics*, 7(1):39–61, 1971.

[29] G C Sih. *Plates and shells with cracks: a collection of stress intensity factor solutions for cracks in plates and shells*, volume 3. Springer Science & Business Media, 2012.

[30] L Slepyan. Forced waves in a uniform waveguide with distributed and localized dynamic structures attached. *International Journal of Engineering Science*, 173:103628, 2022.

[31] M L Williams. The bending stress distribution at the base of a stationary crack. *J. Appl. Mech.*, pages 78–82, 1961.

[32] Haiying Zhang, Zhenwen Zhou, Alexander Chudnovsky, and Hoang Pham. Time-dependent buckling delamination of thin plastic films and their conformability: Observations and modeling. *International Journal of Engineering Science*, 150:103258, 2020.

[33] Z. Zhuang, Z. Liu, B. Cheng, and J. Liao. *Extended finite element method*, chapter X-FEM on Continuum-Based Shell Elements. Tsinghua University Press computational mechanics series. Tsinghua University Press, Beijing, 2014.

**Declaration of interests**

☐The authors declare that they have no known competing financial interests or personal relationships that could have appeared to influence the work reported in this paper.

☒The authors declare the following financial interests/personal relationships which may be considered as potential competing interests:

| |
|---|
| Andrea Nobili reports financial support was provided by Government of Italy Ministry of Education University and Research. Gennady Mishuris reports a relationship with European Union that includes: funding grants. |